

UC Irvine

Faculty Publications

Title

Constraining MODIS snow albedo at large solar zenith angles: Implications for the surface energy budget in Greenland

Permalink

<https://escholarship.org/uc/item/366856zj>

Journal

Journal of Geophysical Research, 115(F4)

ISSN

0148-0227

Authors

Wang, Xianwei
Zender, Charles S

Publication Date

2010-11-06

DOI

10.1029/2009JF001436

Copyright Information

This work is made available under the terms of a Creative Commons Attribution License, available at <https://creativecommons.org/licenses/by/4.0/>

Peer reviewed

1
2 **Constraining MODIS snow albedo at large solar zenith angles: Implications for surface energy**
3 **budget in Greenland**
4

5
6 Xianwei Wang, Charles S. Zender
7

8 Department of Earth System Science, University of California, Irvine, USA
9
10
11
12
13
14
15
16
17
18
19
20
21
22
23
24
25
26
27
28
29
30
31
32
33
34
35
36
37
38

39 Corresponding Author: Xianwei Wang

40 Email: xianweiw@uci.edu ; xianwei8.wang@gmail.com

41 Tel: 1-949-824-1571

42 Fax: 1-949-824-3874
43

44 **Abstract**

45 An understanding of the surface albedo of high latitudes is crucial for climate change studies. MODIS albedo retrievals
46 flagged as high quality compare well with *in situ* Greenland Climate Network (GC-Net) measurements but cover too little
47 area to fully characterize Greenland's albedo in non-summer months. In contrast, poor quality MODIS retrievals provide
48 adequate spatio-temporal coverage, but are not recommended for use at large solar zenith angles (SZAs) where they have a
49 systematic low bias. We introduced an empirical adjustment to the poor quality data based on high quality reference albedos
50 and constrained by GC-Net data and theory, and used the adjusted data to improve estimates and fill-in gaps of the year-
51 round, Greenland-wide, albedo and surface energy budget. For observations made with SZAs between 55° and 75°, the
52 mean differences (MODIS minus GC-Net) between our adjusted MODIS albedo and GC-Net measurements are -0.02 and
53 -0.03 at Saddle and Summit, respectively, compared to -0.05 and -0.08 between the unadjusted MODIS albedo and GC-Net
54 measurements. The adjusted MODIS snow albedos are usually between 0.75 and 0.87 over dry snow when SZA is larger
55 than 55°, and they reduce unrealistic seasonal and meridional trends associated with MODIS retrievals at large SZA,
56 defined as $SZA > 55^\circ$ and 70° , respectively, for low- and high-quality retrievals. The impact of the adjusted albedo on the
57 surface energy budget, relative to the unadjusted albedo from all MODIS data, is least ($-0.7 \pm 0.1 \text{ W/m}^2$) in June, and greatest
58 ($-6.2 \pm 0.9 \text{ W/m}^2$) in September for the black-sky albedo (BSA). The mean annual absorbed solar radiation (ASR) reduction
59 by the adjusted MODIS albedo in Greenland from 2003 to 2005 is 3.1 ± 0.2 and $4.3 \pm 0.2 \text{ W/m}^2$ for BSA and white-sky
60 albedo (WSA), respectively, about $8.0 \pm 0.5\%$ and $10.8 \pm 0.4\%$ of ASR based on the raw BSA and WSA. The ASR reduction
61 by the adjusted blue-sky (actual) albedo is between 2.9 and 4.5 W/m^2 , enough to annually melt 27.1 to 41.7 cm snow water
62 equivalent (SWE), or to sublimate 3.2 to 4.9 cm SWE. The ASR difference between the adjusted MODIS BSA and CERES
63 albedo in March from 2003-2005 is only $-0.1 \pm 0.9 \text{ W/m}^2$, much less than the difference ($4.9 \pm 1.4 \text{ W/m}^2$) between the
64 unadjusted MODIS BSA and CERES. The albedo adjustments exceed the likely direct anthropogenic radiative forcing
65 experienced by Greenland due to greenhouse gases or aerosols. The proposed adjustment preserves most of the zonal and
66 meridional structure of raw MODIS albedo, and extends its usefulness as a cryospheric climate record in times and regions
67 of Greenland with large SZA.

68

69 **KEY WORDS: MODIS; Snow Albedo; Solar Zenith Angle; Greenland; Surface Energy Budget**

70 1. Introduction

71 Snow covers most of Greenland year-round, and thus plays a pivotal role in determining the surface
72 energy balance of Greenland which, by virtue of its area, ice-volume, and location near regions of
73 North Atlantic deep-water formation, plays an important role in the climate system (Steffen and Box,
74 2001). The minimum (summer solstice) Solar Zenith Angles (SZAs) in southernmost and
75 northernmost Greenland are 37° and 60° , respectively. Such high SZAs pose serious challenges not
76 only to *in situ* solar radiation measurements (Augustine et al., 2000), but also to the consistency and
77 accuracy of the MODerate resolution Imaging Spectroradiometer (MODIS) surface albedo retrieval
78 algorithms applied to polar regions (Lucht, 1998; Liu et al., 2009). Due to its length (about 10 years)
79 and relatively high spatio-temporal resolution (500 m pixels every eight days), the MODIS-retrieved
80 surface reflectance has become a valuable climate data record for monitoring and evaluating the
81 significance of snow albedo, and thus surface energy, changes in remote regions.

82 Theoretically snow surface albedo increases with SZA because the increased path over which
83 obliquely-incident photons may interact with the snow grains allows more multiple scattering and less
84 penetration through or absorption by snow. This results in a larger fraction of oblique solar radiation
85 reflected by snow (Wiscombe and Warren, 1980; Warren, 1982; Lucht, 1998; Wang et al., 2005).
86 Several field studies show surface albedo increases with SZA over snow, desert, and vegetated surfaces
87 (Warren and Wiscombe, 1980; Jin et al., 2003b; Wang et al., 2005; Liu et al., 2009). Although the
88 MODIS albedo increases with the SZA increase at low SZA (Lucht, 1998; Jin et al, 2003b), Liu et al.
89 (2009) document an increasingly negative bias at the Atmospheric Radiation Measurement Southern
90 Great Plains (ARM/SGP) stations as SZA increases beyond 70° .

91 Previous studies show that the broadband shortwave albedos for dry snow generally span the
92 range from 0.81 to 0.85 at South Pole when $\text{SZA} > 66^\circ$ (Kuhn and Siogas, 1978; Carroll and Fitch,
93 1981). The Greenland climate network (GC-Net) measurements agree with this range, with measured

94 snow albedo larger than 0.8 as $\text{SZA} > 60^\circ$. In contrast, the MODIS-retrieved snow albedos in areas of
95 Greenland known to be covered with dry snow dip as low as 0.6 for $\text{SZA} > 70^\circ$ for the magnitude
96 inversions (quality flag $Q>0$) while theory and GC-Net measurements show that the snow albedo
97 remains unchanged or increases slightly as SZA increases (Wang and Zender, 2010). It must be noted
98 that Wang and Zender (2010) did not discriminate the retrievals by quality flag. More careful analysis
99 shows that the biases they identified are attributable to poor quality retrievals for $55^\circ < \text{SZA} < 70^\circ$
100 (where the high quality retrievals perform well), and by all retrievals for $\text{SZA} > 70^\circ$, which is beyond
101 the recommended range of use of the albedo product (Stroeve *et al.*, 2005). Liu et al. (2009) attribute
102 the decline of the MODIS albedo with large SZA to the extrapolation algorithm and/or to the
103 Bidirectional Reflectance Distribution Function (BRDF) model over snow surfaces. Wang and Zender
104 (2010) concluded that the accuracy of MODIS albedos deteriorates for $Q>0$ data when $\text{SZA} > 55^\circ$ and
105 for $Q=0$ data when $\text{SZA} > 70^\circ$ and that these albedos can be physically unrealistic for $\text{SZA} > 70^\circ$.
106 Many studies intercompare GCM modeled albedo results with the combined (comprising both high-
107 and low-quality retrievals) MODIS dataset (Zhou et al., 2003; Oleson et al., 2003; Roesch 2006). These
108 earlier uses of the combined MODIS dataset were more exploratory, and their comparisons over
109 Greenland, Antarctica, and other high latitude snow-covered regions should be re-considered in light of
110 subsequent studies that document low biases at large SZA (Stroeve et al., 2005; Liu et al., 2009; Wang
111 and Zender, 2010).

112 Despite the problems noted above with retrieved snow albedos for $\text{SZA} > 55\text{--}70^\circ$, an extensive
113 literature search finds good agreements between the MODIS-estimated surface albedo and *in situ*
114 observations. At most Surface Radiation Budget Network (SURFRAD) sites, the overall absolute
115 accuracy of MODIS albedo is within 0.05 and shows an increasing negative bias and increasing root
116 mean square error (RMSE) compared to ground observations as SZA increases beyond 70° (Liu et al.,
117 2009). At the Gaize Automatic Weather Station on the western Tibetan Plateau with semi-desert or

118 desert soil, the MODIS albedo does not show a distinctive bias with the ground-measured albedo
119 (Wang et al., 2004). At the SURFRAD sites and Cloud and Radiation Testbed-Southern Great Plains
120 (CART/SGP) sites, the MODIS surface albedo generally meets an absolute accuracy requirement of
121 0.02 with an RMSE less than 0.018 during April-September 2001 (Jin et al., 2003b). In snow-free
122 periods, MODIS albedo shows good agreements with worldwide Baseline Surface Radiation Network
123 (BSRN) measurements (Rose et al., 2004). At perennially snow-covered sites in Greenland, MODIS
124 retrieves snow albedo with an RMSE of 0.04 for high-quality retrievals and 0.07 for all retrievals with
125 $SZA < 70^\circ$ in 2000-2003, relative to GC-Net measurements, which have an RMSE of 0.035 relative to
126 the BSRN measurements at Summit (Stroeve et al., 2005). Moreover, MODIS snow albedos at large
127 SZAs are self-consistent and are likely to capture the underlying spatial morphology, especially its
128 zonal features.

129 Greenland receives 46% and 12% of its annual insolation at $SZA > 55^\circ$ and 70° , respectively.
130 Yet the best quality ($Q=0$) MODIS data cover less than 40% of Greenland on each day, and annually
131 only 33% of all retrievals on days 41-297, 2005, when the majority (56%) of retrievals were quality
132 level $Q=2$ data (11% are for data whose $Q=1, 3$, and 4). The best quality ($Q=0$) data congregate near
133 smaller SZAs, i.e., towards southern Greenland and in less-cloudy months (e.g., May and August),
134 when the best quality data is near 50% of all retrievals. The areal fractions of Greenland with the best
135 quality data coverage in March, April, and May, are 13%, 30%, and 36%, respectively. Using data
136 from all quality levels ($Q=0-4$) increases these monthly areal coverages to 80%, 93%, and 98%
137 respectively. For Greenland north of 72° (i.e., north of Summit, which includes about 48% of
138 Greenland's total area), the best quality data coverages in March, April, and May drop to 3%, 24%, and
139 35%, respectively, and utilizing lower quality data increases these to 75%, 91%, and 97%, respectively.
140 Since restricting our analysis to only those cells that are of best quality would eliminate too much data,
141 we use all of the data, as in Oleson et al. (2003), to obtain a full spatial and temporal coverage in

142 Greenland.

143 Our goal is to ensure that the community of scientists interested in surface processes in the
144 cryosphere, and Greenland in particular, becomes aware of the importance of retrieval quality in
145 assessing MODIS snow albedo and of the existence of the MODIS snow albedo bias at large SZAs
146 (defined as $SZA > 55^\circ$ and 70° for low- and high-quality retrievals, respectively) and gains a good
147 sense of its magnitude in Greenland (where we have data to evaluate it) and its implications there for
148 surface processes such as sublimation or snow melt. The strategy we pursue to increase the usefulness
149 of MODIS snow albedo to this community of researchers is to develop empirical adjustments that
150 retain the accurate MODIS retrievals up to $SZA = 55^\circ$, rely on high quality retrievals where possible
151 for SZA between 55° and 70° , and mitigate the large SZA bias elsewhere. We first describe the
152 patterns of the low-bias in MODIS snow albedo at large SZA in Greenland. Then we develop an
153 empirical model to adjust the archived MODIS albedo at large SZA in order to improve its usefulness
154 as a cryospheric climate record. Finally, we evaluate the corrected MODIS albedo using *in situ*
155 measurements and Clouds and the Earth's Radiant Energy System (CERES) surface albedo, and
156 demonstrate its implications for the surface energy budget in Greenland.

157

158 **2. Study Area and Data**

159 **2.1 Study Area and GC-Net Albedo**

160 The Greenland ice sheet is an ideal target to study snow and ice albedo from satellites and has
161 been used as such in several studies (Knap and Oerlemans, 1996; Stroeve et al., 1997, 2001,
162 2005&2006; Greuell and Oerlemans, 2005). First, Greenland has about 20 solar radiation monitoring
163 stations that sample different snow zones. Second, the vast majority of Greenland is perennially snow-
164 covered without the disturbance of vegetation. Third, outside the (increasing) melt-zone (Tedesco,
165 2007), the relatively homogeneous snow surface minimizes the inevitable sampling mismatches

166 between the *in situ* footprint and the satellite areal retrieval. Fourth, Greenland is far downwind from
167 extensive human activities and dust sources. Concentrations of black carbon impurities, the most
168 important absorbing impurity in present day Greenland, are less than 15 ppb and are thought to reduce
169 broadband albedo by less than 1% (Flanner et al., 2007, Table 2). Fifth, Greenland's year-round high
170 reflectivity in the midst of the dark North Atlantic Ocean plays an important role in the polar climate
171 and in fresh water storage. Greenland's surface climatology and geographic features are documented
172 by Steffen and Box (2001).

173 There are 21 GC-Net Automatic Weather Stations (AWS) in Greenland (Figure 1), which
174 provide downwelling and upwelling shortwave irradiance measurement. Five stations (Humboldt GI-
175 HMG, NGRIP-NGR, Summit-SMM, Saddle-SDL and South Dome-SDM) are selected in this study
176 (Table 1). These five stations are located along the crest of the ice sheet and span Greenland from
177 south to north at elevations close to or above 2000 m. Restricting our study to dry snow regions ensures
178 that snow-melt does not contribute to the discrepancy between *in situ* and satellite-retrieved albedos.
179 The GC-Net measurements are available at <http://cires.colorado.edu/science/groups/steffen/gcnet/>.

180 The GC-Net shortwave solar downwelling and upwelling radiation are measured using a pair of
181 horizontally leveled LI-COR 200SZ pyranometers in a narrow spectral range (0.4-1.1 μm) sampled at a
182 15-s interval and averaged over an hour. The LI-COR measurements have 5% uncertainties. The
183 downwelling shortwave solar radiation value measured by a LI-COR 200SZ pyranometer is factory-
184 calibrated to equal the spectral response from 0.28-2.8 μm measured by a more accurate Eppley
185 Precision Spectral Pyranometer (PSP) (LI-COR, 2005; Stroeve et al., 2005). The PSP measures over
186 98% of the downwelling shortwave solar radiation.

187 The LI-COR pyranometers are calibrated against Eppley PSP measurements based on the
188 spectral distribution of the downwelling solar radiation under clear sky. Thus systematic positive biases

189 may exist in the GC-Net measured upwelling irradiances since the snow surface reflects over 90% of
190 the visible solar radiation and depletes most radiation beyond 1.1 μm . Stroeve et al. (2005) compared
191 the solar fluxes measured by LI-COR and Eppley pyranometer at Swiss Camp in Greenland, and found
192 the upward and downward shortwave irradiance errors measured by LI-COR pyranometers did not
193 exceed 2.7%. To compensate for the bias in the reflected LI-COR 200SZ pyranometer measured
194 irradiances, they corrected the GC-Net albedo with a site-specific albedo offset ranging from 0.01 to
195 0.09. Because the snow albedo discrepancies against the precise pyranometer measurements vary
196 greatly among different calibration sites reported in Stroeve et al. (2005), and because the uncorrected
197 GC-Net measured snow albedo values at the five stations that we consider fall in a similar range as
198 those precise pyranometer measurements, and in order to avoid additional site-specific uncertainties
199 due to correcting the GC-Net snow albedo, none of the downward or the upward irradiance data are
200 adjusted in this study. The potential positive bias in the GC-Net snow albedo must be borne in mind
201 when comparing to the MODIS-retrieved albedo. To avoid unexpected instrumental errors, we apply
202 an outlier check for the hourly data such that albedo dropping more than 10% against the mean of the
203 two neighboring hours when $\text{SZA} < 80^\circ$ is replaced by the mean or discarded as non-credible data.

204 In order to compare with the local noon MODIS albedo, the daily *in situ* albedo is derived from
205 the average of shortwave downwelling and upwelling irradiance within a three-hour period centered on
206 local noon (11:00, 12:00 and 13:00). The 16-day albedo is derived from the daily average of
207 downwelling and upwelling solar radiation in clear skies for each 16-day period of MODIS albedo.
208 Clear sky is defined when the cloud cover fraction at the MODIS gridpoint coincident with the GC-
209 Net site is less than 10% according to the daily snow cover product (MOD10C1), which contains the
210 cloud cover fraction (Wang et al., 2008).

211

2.2. MODIS Albedo

The MODIS instruments aboard both NASA's Terra and Aqua satellites acquire daily images and provide global land surface albedos that include the daily unvalidated beta-test albedo product and the 16-day validated standard product (Schaaf et al., 2002; Stroeve et al., 2006). The MODIS standard 16-day surface albedo products are produced every 8 days within 16 days of acquisition. There are multi-angle observations in the 16-days. If the majority of observations are recorded as snow-covered, then the algorithm uses only snow-covered observations for the parameter retrievals; otherwise, the algorithm conservatively uses snow-free observations for parameter retrievals (Schaaf et al., 2002; Salomon et al., 2006). Meanwhile, if there are at least seven cloud-free observations during the 16 days, a full model inversion or the “main” algorithm is attempted; otherwise, a magnitude inversion or the “backup” algorithm is performed (Schaaf et al., 2002). MODIS albedo products provide directional hemispheric reflectance (black-sky albedo, BSA) and bihemispheric diffuse reflectance (white-sky albedo). Each BSA and WSA include seven narrow spectral bands (MODIS band 1-7) and three broadband (0.3-0.7, 0.7-5.0, 0.3-5.0 μm). The broadband albedos are converted from the spectral reflectance via a narrow-to-broadband conversion factor (Liang et al., 1999; Stroeve et al., 2005). The shortwave broadband (0.3-5.0 μm) albedo (hereinafter referred to as MODIS albedo) has the best spectral match to most broadband instruments and is of the greatest interest to climate studies because it determines the net surface solar radiation flux. The actual albedo (also called blue-sky albedo) is a solar flux-weighted average of the intrinsic black-sky albedo and white-sky albedo, where the proportion of direct and diffuse solar radiation depends on the atmospheric conditions and SZA, usually reported at local noon for MODIS (Lewis and Barnsley, 1994; Schaaf et al., 2002). The MODIS Terra and Aqua combined albedo products have higher quality retrievals than Terra-only albedo products (Salomon et al., 2006).

The MODIS Terra and Aqua combined albedo has been available since Aqua MODIS

236 operational retrievals began in June 2002. MODIS albedo products come in two grids and are
237 distributed by the NASA Land Process Distributed Active Archive Center (LP DAAC) at
238 https://lpdaac.usgs.gov/lpdaac/get_data/wist. One is a sinusoidal projection with 500 m and 1 km
239 spatial resolution, and the other is the climate modeling grid (CMG) at 0.05 degree (about 5.6 km near
240 the equator), which is aggregated from the 500 m product. Following Wang et al. (2005), this study
241 uses the combined 0.05 degree MODIS albedo product (MCD43C3) from 2003 to 2007. MCD43C3
242 contains WSA and BSA for 7 spectral bands and three broadbands, snow cover fraction (SCF), local
243 noon solar zenith angle (SZA), and the BRDF quality code. The quality flag has five values for the
244 aggregated 0.05° product in MCD43C3. Q=0 represents the best quality and indicates that 75% or
245 more of the 500 m pixels that compose the aggregated point were retrieved with the full inversion
246 algorithm; Q=1 points are good quality, though less than Q=0 quality, and are also composed of 75%
247 or more full inversions; Q= 2 means mixed quality, comprising fewer than 75% full inversions and
248 fewer than 25% fill values; Q=3 suggests all magnitude inversions with fewer than 50% fill values;
249 while aggregated points with Q=4 include more than 50% fill values. For near-homogeneous bright
250 snow surfaces, both BSA and WSA are similar, and each closely represents the blue-sky albedo when
251 SZA is less than 55°(Stroeve et al., 2005; Wang and Zender, 2010). This study reaches similar
252 conclusions from independent analyses of BSA and WSA data, and occasionally, for brevity, we
253 illustrate our results for BSA only.

254 The albedo at one MODIS gridpoint (5.6 km x 0.8-2.8km in Greenland) centered on each of the
255 five stations is used to compare with GC-Net measurements. The MODIS albedo difference between
256 one gridpoint and a square of 3x3 gridpoints at the near uniform snow surface in Greenland is
257 negligible. The point scale *in situ* measurements are assumed to represent the ground truth of the areal
258 value of one MODIS grid, e.g., ~5.6 km x 1.68 km at Summit, 72.5°N. Although the near-
259 homogeneous snow cover and relatively flat surface may minimize the point-areal discrepancy (Jin et

260 al., 2003b), any conclusion about the accuracy of the MODIS albedo must consider this and the
261 uncertainties of the *in situ* shortwave downwelling and upwelling radiation measurements.

262

263 **2.3. CERES albedo**

264 Like MODIS, the Clouds and the Earth's Radiant Energy System (CERES) instrument is
265 aboard both Terra and Aqua satellites. CERES measures broadband shortwave solar radiances at the
266 Top Of Atmosphere (TOA), while MODIS measures narrow-band radiances in various shortwave
267 bands (Jin et al., 2008). CERES generates global 1° gridded Monthly TOA/Surface Averages
268 (SRBAVG) datasets. This study uses the CERES Terra FM2 Edition2D SRBAVG, which infuses
269 observations from Geostationary Narrowband Radiances (GEO) and MODIS cloud data products and
270 represents the most robust CERES TOA/surface monthly mean flux product (Wielicki, et al., 1996).
271 The surface fluxes are calculated using parameterizations based on TOA fluxes, cloud properties and
272 GEO-based atmospheric vertical model profiles. The global 1° gridded monthly shortwave (SW 0.2-5
273 μm) surface downwelling and net fluxes in the SRBAVG product are simply resampled into the global
274 0.05° CMG grid for comparison with the MODIS albedo product. The SRBAVG product is generated
275 for a period from 2000 to 2005 at present, and only the data from 2003 to 2005 are used for comparison
276 with the MODIS albedo and for the surface energy flux analysis.

277

278 **3. Results**

279 **3.1 MODIS Albedo Bias**

280 Before introducing the proposed correction to MODIS albedo at high SZA, it is instructive to
281 summarize how albedo changes with large SZA in both temporal and spatial dimensions. At a given
282 location, like Summit, the SZA is smallest at sidereal noon in the diurnal cycle, and in summer for the

283 seasonal cycle. At a given day or time, SZA is smaller at a lower latitude. Wang and Zender (2010)
284 document the theoretical and observed behavior of snow albedo (both GC-Net and MODIS) in dry
285 snow regions of Greenland on the diurnal, seasonal, and inter-annual timescales. They show that
286 temporally, over dry snow-covered regions of Greenland, the MODIS snow albedo ($Q>0$) decreases
287 steeply as SZA exceeds 55-60°, and can reach values below 0.6 when $SZA > 75^\circ$. Our proposed albedo
288 adjustment takes advantage of our new finding (Figure 2) that these albedo decreases correlate
289 positively and significantly with the cosine (SZA) in all years examined for both spring and fall at
290 Summit. The SZA cosine explains 24-89% of the variance in BSA decline for large SZA at Summit. At
291 vegetated (grassland with few trees) SURFRAD sites, the negative bias of MODIS albedo also
292 increases as SZA increases beyond 70° (Liu et al., 2009). Other stations and years behave similarly to
293 Summit for both BSA and WSA (not shown). Regressions and variance explained (R^2 values) are
294 computed separately in spring and fall at each station and in each year in order to preserve any
295 difference due to different seasonal properties of snow. In each season, there are only seven or eight
296 data points available for SZA from 55° to 75° (recall that MODIS albedos are provided every eight
297 days). Because of the limited data in each season, each datum has a strong influence on the final R^2
298 value. As a result, the regression coefficients vary greatly. Linear fits are better (higher R^2) in the fall
299 than in the spring.

300 Spatially, the correlation coefficients (Figure 3) between the zonal mean (longitude 50°W -
301 40°W) BSA within one-degree latitude bands from 65°N to 80°N and $\cos(SZA)$ on each day are
302 significant and positive when the SZA at 65°N exceeds 50°. The albedo differences between latitude
303 65°N and 80°N are indistinguishable in warm months, but the differences increase to 0.18 in cold
304 months. The raw MODIS monthly snow albedo (BSA) map in March 2005 (other years and WSA, not
305 shown, are similar) shows the decreasing albedo trend towards northern Greenland (Figure 4b). The

306 flux and area-weighted mean snow albedo in Greenland in March, 2005 is 0.06 less in MODIS than in
307 CERES (Figure 4c). Regionally, the low-bias in MODIS relative to CERES albedo increases up to 0.2
308 at latitudes $> 75^{\circ}\text{N}$ (Figure 4c). The lower surface albedo implies that the surface Absorbed Solar
309 Radiation (ASR) is, on average, 5.18 W/m^2 greater for MODIS than CERES (Figure 4d). This ASR
310 difference is about 23% of the ASR implied by the raw MODIS albedo, and 6% of the surface
311 downwelling solar insolation. In spite of its potential uncertainty (overestimate at latitudes $> 75^{\circ}\text{N}$) and
312 coarser spatial resolution, CERES snow albedo increases with latitude and SZA (Figure 4a) as
313 predicted by theory and as seen in *in situ* measurements (Wang and Zender, 2010).

314 In summary, Figures 2-4 and Table 2 demonstrate that MODIS snow albedo (constructed from
315 all quality level retrievals) has a systematic negative bias at large SZA ($>55\text{-}60^{\circ}$). This bias is closely
316 related to SZA, and in particular for the magnitude inversions with $Q>0$ at large SZA. The Greenland-
317 wide MODIS albedo is credible during June and July and with the best full inversions ($Q=0$) which
318 appear unbiased for $\text{SZA} < 70^{\circ}$. However, $Q=0$ retrievals comprise only 35% of the retrievals in June
319 and July in Greenland, and congregate towards smaller SZAs, i.e., southern Greenland. The sparsity of
320 high quality retrievals at large SZA means that all retrievals must be used to realize the full spatio-
321 temporal coverage afforded by MODIS.

322

323 3.2 Proposed Albedo Correction

324 We propose a short-term empirical method to mitigate the MODIS albedo bias and to quantify
325 its implications on the surface energy budget, from which the climate/cryosphere community would
326 benefit. The theoretical dependence of spectral snow albedo on SZA, snow grain size and three single-
327 scattering properties is well-known and has been expressed analytically in the delta-Eddington
328 approximation (Wiscombe and Warren, 1980). The required inputs for that expression are unavailable

in practice, so we start from an empirical surface albedo representation that depends on SZA and one free parameter (Dickinson, 1983; Briegleb et al., 1986; Wang et al., 2005).

$$A(\theta) = A(\theta_0) \times \frac{1+C}{1+2C \times \cos(\theta)} \quad (1)$$

where A is the black-sky albedo, θ is SZA, θ_0 is the reference SZA (usually near 60°), and $A(\theta_0)$ is the albedo at the reference SZA which depends on date and location, and C is a surface-dependent empirical parameter of order 0.1.

Though equation (1) has been widely used in modeling land surface solar fluxes (Pinker and Laszlo et al., 1992) and land-atmosphere coupled models (Briegleb et al., 1986; Kiehl et al. 1998, Hou et al., 2002), it cannot directly incorporate the MODIS retrieved albedo for $\text{SZA} > \theta_0$ and we would like to retain the spatial morphology of MODIS retrieved albedos for large SZA. We consider five factors in modifying Equation (1) to fit our needs. First, no adjustment should be made where the raw MODIS snow albedo is presumed to be robust ($Q=0$ & $\text{SZA} < 70^\circ$, and $Q>0$ & $\text{SZA} < 55^\circ$), and these robust data should be used, where and when available, to adjust the non-robust data. Second, where adjustments are made, they should be consistent with *in situ* observed dry snow albedo at large SZA. Third, the adjustment should be consistent with the SZA contribution to snow albedo at large SZA. Fourth, the adjustment should retain, when possible, spatial morphology of the raw MODIS albedo. Fifth, adjustments should not be made when non-snow or wet snow surfaces are indicated. To address these issues, we propose Equation (2) to adjust the raw MODIS snow albedo at large SZA:

$$A'(\theta) = A(\theta) + (\bar{A}_0 - A(\theta)) \times \frac{1+C}{1+1.74C \times \cos(\theta)} \quad (2)$$

Here $A(\theta)$ is the raw MODIS retrieved albedo at θ SZA, and \bar{A}_0 is the reference albedo, taken to be the zonal mean albedo at the reference SZA (55°) for 100% snow-covered gridpoints. Thus, \bar{A}_0

varies with date and location. Since we set the reference SZA to 55° in Equation (2), we also changed the coefficient of C in Equation (1) to 1.74 to guarantee that the adjusted albedo ($A'(\theta)$) increases with SZA. Correspondingly, C is changed to 0.15 for pure snow cover. This value constrains the total snow albedo increase caused by a 25° SZA increase from 55° to 80° to 0.04, in agreement with GC-Net observations and model simulations (Wang and Zender, 2010).

In Equation (2), the reference albedo, \bar{A}_0 , is the most critical parameter. It is computed in one of two ways. When the SZA at latitude 63°N ($\text{SZA}_{63\text{N}}$) is less than 55° (e.g., from day 105 to day 241 in Greenland), then \bar{A}_0 is the zonal mean albedo at $\text{SZA}=55^\circ$. When $\text{SZA}_{63\text{N}}$ is larger than 55° (e.g., before day 105 and after day 241), then \bar{A}_0 is taken as the zonal mean albedo at latitude 63°N , and if this value is less than 0.8 then it is further adjusted by Equation (3) below. We choose the reference SZA = 55° because MODIS snow albedo is largest, and is still robust even for the magnitude inversions, at this SZA (Liu et al., 2009; Wang and Zender, 2010). This choice is also consistent with Petzold's (1977) empirical rule-of-thumb that snow albedo is virtually independent of SZA for SZA $< 50^\circ$. \bar{A}_0 is the average albedo of all 100% snow-covered gridpoints of the best ($Q=0$) retrievals whose noontime SZA = 55° (or, if $\text{SZA}_{63\text{N}} > 55^\circ$, whose latitude is 63°N), and whose albedo is greater than 0.75 on the day of the adjustment. The albedo threshold of 0.75, which is derived from the MODIS best retrieval snow albedo in June and July, for contributing to \bar{A}_0 sets a minimum adjusted snow albedo when SZA = 55° . We choose latitude 63°N as the southernmost point to calculate the reference albedo when $\text{SZA}_{63\text{N}}$ is larger than 55° because it is near South Dome (63.15°N , 44.81°W), the southernmost GC-Net station that is perennially snow-covered. However, the MODIS reference albedo at 63°N is often relatively too dark (< 0.8) because the large SZA ($> 65^\circ$) there produces an artificially low raw MODIS albedo that itself must be adjusted. Thus we adjust any $\bar{A}_0(63^\circ\text{N}) < 0.8$ before use in Equation (2) by applying Equation (3) which uses a ramp function to remap the reference

373 albedo so that $\bar{A}_0 > 0.8$ when $SZA_{63N} > 55^\circ$.

$$\bar{A}_0 = \bar{A}(63N) \quad \text{for } \bar{A}(63N) \geq 0.8 \quad 3a$$

$$\bar{A}_0 = 0.8 + (0.8 - \bar{A}(63N)) \times 0.15 \quad \text{for } 0.75 \leq \bar{A}(63N) < 0.8 \quad 3b$$

$$374 \quad \bar{A}_0 = 0.82 \quad \text{for } \bar{A}(63N) < 0.75 \quad 3c \quad (3)$$

375 Equation (3) is applied only if $SZA_{63N} > 55^\circ$ (e.g., before day 105 and after day 241) and produces

376 \bar{A}_0 consistent with GC-Net measurements at South Dome. In practice, Equation (3b&c) is only

377 applied when $SZA_{63N} > 65^\circ$ because mean albedo for best retrievals at $63^\circ N$ is larger than 0.8 when

378 SZA_{63N} is less than 65° . \bar{A}_0 generally increases with SZA since $\bar{A}(63N)$ from MODIS decreases

379 with SZA as $SZA > 65^\circ$.

380 Equation (2) adjusts the original MODIS retrieved albedo $A(\theta)$ by an offset scaled to the

381 albedo difference between \bar{A}_0 and $A(\theta)$. In practice we apply equation (2) only at gridpoints that meet

382 five conditions: (1) SCF=100%, (2) $A(\theta) < \bar{A}_0$, (3) $Q > 0$ & $SZA > 55^\circ$ or $SZA > 70^\circ$, (4) $A(\theta)$ is

383 between 0.5 and 0.8, and (5) SCF=100% at the same grid but on day 161. The last three conditions help

384 to exclude wet or melted snow by only allowing corrections at perennially snow-covered gridpoints.

385 The original MODIS snow albedo is not adjusted when any one of the above five conditions is not

386 satisfied. This occurs mainly in the warm months in June and July. [Condition \(3\) preserves the best](#)

387 [retrieval \(\$Q=0\$ \) MODIS snow albedo for \$SZA < 70^\circ\$, and adjusts the albedo, using raw data of all](#)

388 [qualities, when \$SZA \geq 70^\circ\$](#) . Finally, we fill-in missing albedos with the mean adjusted albedo at the

389 same latitude.

390 The maximum adjusted snow albedo produced by this algorithm is 0.87. A fresh dry snow

391 albedo of 0.87 under clear skies is consistent with Stroeve et al. (2005). The lower bound on the

392 adjusted snow albedo allowed by this algorithm is 0.75, which is also the lower bound of the reference

393 albedo, and is consistent with the best retrieval snow albedo in Greenland in summer months.

394

395 3.3 Model Sensitivity Analysis

396 We now consider the sensitivity of the bias-adjustment procedure to choices made in its
397 formulation. First we examine the behavior of different candidates for the reference albedo in Equation
398 3 (Figure 5); then we examine the effects of different reference albedos on the adjusted albedo at
399 Summit (Figure 6); last, we demonstrate the sensitivity of the corrected albedos to different C values
400 (Figure 7).

401 Recall that the adjustment algorithm (2) employs as the reference albedo (\bar{A}_r) either the zonal
402 mean albedo at $\text{SZA} = 55^\circ$, or the (possibly adjusted) zonal mean albedo at latitude $= 63^\circ\text{N}$. Figure 5
403 compares the temporal variation of the reference albedo (red curve) employed in 2005 to the
404 unadjusted zonal mean albedo at latitude 63°N (green curve). The temporal variation of these albedos
405 are quite similar, and are much the same for both WSA and BSA in 2005 (other years, not shown, are
406 similar). The reference albedo employed is usually (especially during warm months) higher than the
407 unadjusted mean albedo at 63°N . The advantage of a reference albedo that migrates in space and time
408 (i.e., with $\text{SZA} = 55^\circ$), over one fixed to a certain latitude (i.e., 63°N) is that the former puts more
409 weight on the MODIS albedo retrievals located closer to those to be adjusted, and this better retains the
410 spatio-temporal variations captured by the raw MODIS albedo.

411 The reference albedo is *always* calculated from the best quality ($Q=0$) retrievals. Between
412 10 and 350 of these $Q=0$ gridpoints compose each \bar{A}_r (Figure 5). The number of $Q=0$ gridpoints used
413 to calculate the reference albedo decreases in warm months when the latitude where $\text{SZA}=55^\circ$ migrates
414 to northern Greenland, and in cold months when this latitude migrates to southern Greenland which is
415 relatively narrow geographically.

416 The corrected albedo at Summit is affected by the choice of reference albedo (Figure 6). In

417 warm months when Summit's SZA $< 55^\circ$ (i.e., days 129-217), the WSA is close to the BSA and no
 418 adjustments are made even though the MODIS albedo is about 10% less than the GC-Net
 419 measurements. Raw WSA and BSA both reach maxima when SZA is around 55° on days 129 and
 420 217/225, and then artificially decrease as SZA increases. Moreover, for SZA larger than 55° , WSA
 421 decreases faster with SZA than does BSA. Our algorithm, Equation (2), adjusts the artificial albedo
 422 decreases before day 129 and after day 217. The adjusted albedo is larger than 0.8 and remains constant
 423 or increases slightly with SZA. On days 105 to 121 and days 225 to 241, the adjustment uses the
 424 reference albedo at SZA= 55° , and the adjusted albedo varies more than it would have had the
 425 unadjusted albedo at 63°N been used as the reference albedo. Before day 105 and after day 241, the
 426 adjustment algorithm uses the albedo at 63°N as the reference albedo. Equation (3b&c) remedies the
 427 artificial decrease of the reference albedo at 63°N and this causes the adjusted albedo increase slightly
 428 with SZA before day 89 and after day 273.

429 The C parameter in Equation (2) determines the magnitude of snow albedo dependence on SZA.
 430 Figure 7 illustrates the sensitivity of the corrected snow albedo to different C values along a south-to-
 431 north transect ($62\text{--}80^\circ\text{N}$, 45°W) in central Greenland on day 73, 2005. On this day the SZA
 432 approximately equals the latitude. The WSA and BSA reference albedos, derived from 83 Q=0
 433 gridpoints, are 0.807 and 0.815, respectively. The adjusted snow albedo, using the recommended C
 434 value of 0.15 in Equation (2), increases along this transect by 0.03 for WSA and 0.02 for BSA as SZA
 435 increases from 65° (at 65°N) to 80° (at 80°N). The adjusted albedos increase slightly, rather than
 436 dropping sharply, for SZA $> 71^\circ$. Raw albedos are only adjusted where they are less than the daily
 437 reference albedo (0.807 and 0.815) and, simultaneously, less than 0.80.

438

439 3.4 Adjusted MODIS Albedo

440 Multiple annual cycles of the adjusted MODIS albedo are shown alongside the raw MODIS
441 albedo and *in situ* GC-Net albedo at Saddle and Summit in Figure 8. For observations made with SZAs
442 between 55° and 75°, the mean differences (MODIS minus GC-Net) between the adjusted MODIS
443 albedos and GC-Net measurements are -0.02 and -0.03 at Saddle and Summit, respectively, compared
444 to -0.05 and -0.08 between the original MODIS albedo and GC-Net observations. Here “mean
445 difference” is the arithmetic mean of the difference between the MODIS albedo and the GC-Net
446 measured albedo. As mentioned above, GC-Net overestimates snow albedo by about 0.03 relative to a
447 limited collection of more precise measurements at Summit (Stroeve et al, 2005). Hence the adjusted
448 MODIS snow albedo which is ~0.03 less than GC-Net measurements is consistent with those more
449 precise measurements. The adjustment is a conservative estimate of snow brightness in Greenland in
450 that it could be up to 0.04 brighter than the reference albedo without exceeding GC-Net measurements.
451 Nonetheless we err on the side of the minimal adjustments necessary to bring MODIS into agreement
452 with other measurements and with theory at large SZA.

453 The geographic distribution of raw and adjusted albedos on two days in March (day 73) and
454 April (day 105) 2005 demonstrates how the adjustment compresses the dynamic range of albedo, while
455 retaining the observed structure, and imposing the theoretically predicted and *in situ*-observed
456 brightening of snow with the increasing SZA (Figure 9). The adjusted snow albedo also preserves the
457 spatial continuity with the raw albedo for SZA less than 55° around the latitude of 65°N on day 105
458 (Figure 9d). On these two days, the raw MODIS snow albedo generally decreases as latitude and SZA
459 increase. The raw values are physically unrealistic (beneath 0.75) over large regions of Greenland.
460 The adjusted albedo damps the physically unrealistic albedo decline of the raw MODIS albedo at large
461 SZA, yet preserves its spatial patterns, and fills in regions of missing data.

462

463 3.5 Surface Energy Budget

464 The increased brightness of the adjusted MODIS snow albedo (BSA) reduces climatological
465 mean (average of 2003 to 2005) monthly ASR by a minimum of $0.7 \pm 0.1 \text{ W/m}^2$ (in June) to a maximum
466 of $6.2 \pm 0.9 \text{ W/m}^2$ (in September), where the uncertainties are indicated as plus/minus one δ , the
467 standard deviation of the three years comprising the climatology (Table 2). These reductions in ASR
468 are, respectively, $0.2 \pm 0.03\%$ and $4.7 \pm 0.7\%$ of the surface downwelling solar insolation and $0.5 \pm 0.1\%$
469 and $21.2 \pm 2.9\%$ of the ASR based on the raw MODIS albedo. The reduction in annual mean ASR is
470 $3.1 \pm 0.2 \text{ W/m}^2$, about $1.9 \pm 0.1\%$ of the surface insolation and $8.0 \pm 0.5\%$ of ASR. The monthly ASR
471 reductions for the corrected WSA vary from 0.8 ± 0.1 to $8.2 \pm 1.1 \text{ W/m}^2$, and the annual ASR reduction is
472 $4.3 \pm 0.2 \text{ W/m}^2$ (not shown). The actual ASR reduction for the blue-sky albedo is between BSA and
473 WSA ASR reductions.

474 Excluding coastal areas with rocks and fractional snow cover, the adjusted MODIS snow
475 albedo in March 2005 is, as a flux and area-weighted average, 0.003 less than the surface albedo
476 estimated by CERES. Note that the CERES albedo exceeds 0.87 north of 75°N (Figure 10a), a fresh
477 dry snow albedo cap under clear skies set by Stroeve et al. (2005). The GC-Net observations at
478 Humboldt and NGRIP (see Figure 1) do not exceed 0.9, and so it is possible that CERES is
479 overestimating some Greenland surface albedos at these very large SZAs. The difference (adjusted
480 MODIS-CERES) in monthly mean ASR in March 2005 is only 0.29 W/m^2 (Figure 10d), much smaller
481 than the 5.18 W/m^2 difference between CERES and the raw MODIS albedos (Figure 4d). The
482 difference shrinks further if one excludes the region ($> 75^\circ\text{N}$) where CERES appears to overestimate
483 albedo. In addition, the CERES albedo is about 0.04 less than the adjusted MODIS albedo over
484 Greenland from June to August (not shown), and is 0.03 higher than the adjusted MODIS albedo in the
485 northern Greenland of above 75°N in February and March from 2003 to 2005. Thus, CERES may

486 overestimate the snow albedo in Greenland in cold months and underestimate it in warm months.

487 In terms of surface processes in Greenland, the MODIS albedo and implied ASR biases have
488 implications for other terms in the surface energy budget (SEB). MODIS albedos are often used to
489 evaluate or constrain modeled albedos (e.g., Zhou et al., 2003; Oleson et al., 2003). Models that agree
490 with a biased albedo from measurements must compensate with energetically equivalent and opposite
491 biases in the non-constrained terms of the SEB. Simulations with the National Center for Atmospheric
492 Research (NCAR) Community Atmosphere Model (CAM) (Flanner et al., 2007) suggest that, on
493 average, the net longwave emission from Greenland remains relatively constant through the year and
494 that the SEB fluxes most likely to compensate for seasonally varying ASR biases are those of latent
495 heat (i.e., the net snow pack sublimation, snow melt) and sensible heat.

496 To illustrate the effects that the MODIS albedo and implied ASR biases would cause in a
497 model, we show the snow melt and sublimation that would occur due to the MODIS ASR bias (Figure
498 11 and Table 2) being fully converted to melt or sublimation. The MODIS albedo has the largest bias
499 in months from November to February, yet the implied ASR bias and the consequent snow phase
500 change is small because of the limited surface solar insolation in Greenland in winter. The strongest
501 potential impacts of the ASR bias on snow phase change occur from March to May and from August
502 to October for both WSA and BSA. The maximum annual potential snow melt due to this ASR bias is
503 40.2 ± 1.5 cm and 28.9 ± 1.8 cm snow water equivalent (SWE) for WSA and BSA, respectively. This
504 represents the maximum potential snow phase change due to the ASR bias because snow melt where
505 SZA is larger than 55° in Greenland is almost impossible before May and after September (Hall et al.,
506 2009), and because some of the ASR bias will be dissipated by other surface processes such as sensible
507 heating of the atmosphere. The maximum sublimation changes due to the ASR bias are 4.7 ± 0.2 cm and
508 3.4 ± 0.2 cm SWE for WSA and BSA, respectively. The actual effect of the ASR bias on snow phase

509 change is probably closer to the potential snow sublimation between the BSA and WSA because the
510 blue-sky snow albedo combines BSA and WSA, and because most of Greenland is below freezing
511 when SZA is larger than 55°.

512 The geographic distributions of the maximum snow phase change due to the MODIS BSA ASR
513 bias are shown for snow melt in August, and for snow sublimation in March, April and September of
514 2005 (Figure 12). The maximum snow sublimation is less than 0.8 cm SWE in most regions of
515 Greenland in March, and less than 2.0 cm SWE in April and September. The potential snow melt in
516 August is up to 20 cm SWE with the larger values occurring in northern (above 72°N) Greenland.
517 Although the Greenland-wide area-weighted mean phase change is relatively small, local potential
518 snow melt and sublimation are comparatively large in regions and months of large ASR bias. The
519 adjusted MODIS snow albedo ameliorates most of the ASR bias, and thus would reduce the implied
520 phase change biases in models constrained by MODIS albedo.

522 4. Discussion and Summary

523 MODIS albedo retrieval algorithms generally work well for the full inversion data ($Q=0$) at low
524 SZA, although the biases in comparison to *in situ* measurements are worse for snow than for other
525 surface types (Jin et al., 2003b; Wang et al., 2004; Rosech et al., 2004; Stroeve et al., 2005; Liu et al.,
526 2009). At large SZA, however, the negative bias of the shortwave MODIS albedo worsens with
527 increasing SZA (Liu et al., 2009, Wang and Zender, 2010). As a result, MODIS reports snow surfaces
528 too dark by up to 30% in absolute albedo as compared to CERES although the CERES may report
529 snow surfaces too bright (~5% in absolute albedo) in Northern Greenland (>75°). The flux and area-
530 weighted, annual mean ASR difference from 2003 to 2005 due to this bias is $3.1 \pm 0.2 \text{ W/m}^2$, and peaks
531 seasonally in September at $6.2 \pm 0.9 \text{ W/m}^2$. These biases prevent robust measurement-based evaluation

532 of climate model albedo predictions over Greenland and possibly in other high SZA snow-covered
533 regions such as Antarctica (Zhou et al., 2003; Oleson, 2003; Rosech et al., 2005).

534 The difficulty of retrieving high quality surface albedos increases with solar zenith angles.
535 More recently, our analysis of MODIS albedo (MCD43C3) in the dry snow covered regions of
536 Greenland (Wang and Zender, 2010) documents a physically unrealistic snow albedo decline for SZA
537 $> 70^\circ$ for the best quality ($Q=0$) data, and for SZA $> 55^\circ$ for lower quality ($Q > 0$) retrievals, also called
538 magnitude inversion retrievals. For these reasons, the MODIS surface albedo science team considers
539 the best retrieval data for SZA $> 70^\circ$ to be suspect, and recommends avoiding use of all magnitude
540 inversion retrievals ($Q>0$) and of the best retrieval ($Q=0$) data for SZA $> 70^\circ$. However, the dearth of in
541 situ measurements means that satellite-based estimates are necessary to characterize surface albedo and
542 its changes in remote polar regions like Greenland.

543 The strategy of this study is to enhance the MODIS poor quality data by using model simulation
544 and *in situ* data from the GC-Net to characterize snow albedos at large SZAs in Greenland and hereby
545 remediate the implied bias in the surface energy budget. The adjustment is based on a semi-empirical
546 parameterization of the surface albedo dependence on SZA (Dickinson,1983; Briegleb et al., 1985;
547 Wang et al., 2005). The adjustment hinges on a reference albedo defined, to ensure robustness, as the
548 mean snow albedo either at SZA= 55° or at latitude 63°N (in Southern Greenland). The dynamic snow
549 reference albedo relies on nearby gridpoints at the same SZA, and preserves the original temporal
550 variation and spatial continuity with albedo retrievals for SZA $< 55^\circ$. The various thresholds in
551 Equation (3) produce physically realistic snow reference albedos consistent with in situ measurements
552 and theory. The adjustment itself (Equation (2)) is the scaled difference between the reference albedo
553 and the raw retrievals, and thus maintains most of the spatial heterogeneity and temporal variation of
554 the raw MODIS retrievals with diminished magnitude. The adjustment algorithm attempts to avoid

555 adjustments in regions influenced by wet snow, vegetation, or exposed rock. However, it is very
556 challenging to determine which MODIS gridpoints have wet or dry snow or melt ponds using the
557 MODIS snow albedo value alone. The influences of some small (several meters) and shallow melt
558 ponds may be negligible for the MODIS (MCD43C3) grid size of 5.6 km x 0.8-2.8 km in Greenland.
559 Here we rely on a threshold albedo of 0.5 to exclude melt ponds, wet snow, or exposed rocks. In
560 addition, snow surface temperature can indicate whether snow is wet or dry. Hall et al. (2009) use -1°C
561 land surface temperature to distinguish “melt” snow from dry snow. The noontime SZA is also anti-
562 correlated with maximum diurnal temperature. When SZA is larger than 55°, the 2-m air temperature
563 in Greenland is usually far below 0°C according to GC-Net measurements. Moreover, the snow
564 surface air temperature is usually much lower than the 2-m air temperature. Thus, the albedo (> 0.5)
565 and SZA (> 55°) thresholds both help ensure that our adjustment is applied only to dry snow
566 gridpoints.

567 The adjusted MODIS snow albedo behaves in a manner consistent with model simulations, GC-
568 Net measurements, and CERES surface albedos. It has a smaller magnitude of spatial variations than
569 the raw MODIS albedo and, to a lesser extent, than the CERES surface albedo. Compared to GC-Net
570 measurements, the corrected MODIS snow albedo is more realistic than the raw MODIS snow albedo
571 and, at latitudes north of 75°N, than the CERES albedo. The raw MODIS albedo derived ASR bias of
572 2.9-4.5 W/m² exceeds the estimated present day direct climate forcings in Greenland due to
573 anthropogenic agents such as CO₂ (1.4 W/m²) and black carbon (BC) aerosol deposition (0.6 W/m²)
574 (Koch and Hansen, 2005; Flanner et al., 2007& 2009). We intend one consequence of our improved
575 estimates of Greenland surface albedo from MODIS retrievals to be an increased signal-to-noise ratio
576 of perturbations to Greenland's surface albedo by such anthropogenic forcing agents. Until and unless
577 this or similar adjustments to MODIS albedo are applied, the detection of such perturbations to surface

578 albedo is best attempted in regions of smaller MODIS albedo uncertainty, i.e., snowy regions of
579 relatively low SZA, and therefore strong surface insolation, such as the Tibetan Plateau, Colorado
580 Plateau, Rocky Mountains, and western European Alps (Flanner et al., 2007; Painter et al., 2007; Ming
581 et al., 2009).

582 The combined data (comprising low- and high-quality retrievals) MODIS large SZA albedo
583 and implied ASR biases have implications for the other terms in the Surface Energy Budget (SEB) in
584 Greenland. The snow melt and sublimation that would occur due to the MODIS ASR bias being fully
585 converted to melt or sublimation are greatest from March to May and from August to October for
586 both WSA and BSA. The actual effect of the ASR bias on snow phase change is probably closer to the
587 potential snow sublimation between the BSA and WSA because the blue-sky snow albedo combines
588 BSA and WSA, and because most of Greenland is below freezing. Overestimating snowpack ASR can
589 also be expected to trigger positive snow-albedo feedbacks such as the snow cover-albedo feedback
590 and snow albedo reductions due to grain growth and atmospheric conditions (Flanner and Zender,
591 2006). Simulations (Flanner et al., 2007) with CAM estimate that about 34% of the annual surface net
592 solar radiation in Greenland converts to latent heat. Thus, we expect that models constrained to agree
593 with the raw MODIS ASR would overestimate snow phase changes by about one third of the
594 maximum snow melt or sublimation shown in Figures 11 and 12.

595 Our empirical adjustment to MODIS albedo is based on snow optical properties and *in situ*
596 measurements over purely snow-covered regions on Greenland. Further examination utilizing *in situ*
597 data is necessary to test whether systematic adjustments would improve MODIS snow albedo in other
598 regions with large SZA such as Antarctica, and in partially vegetated regions like North America and
599 Eurasia. Other regions may require different formulations for an adjustment algorithm due to regional
600 variations in snow condition and structure (e.g., Sturm et al., 1995). While the adjustment improves, on

601 average, the agreement between non-robust MODIS retrievals with GC-Net and theory, the adjustment
602 is based only on a correlation between SZA and the bias (Figure 2, Equation 2) and so cannot be said to
603 fix the unknown root causes of the bias. Causes of snow albedo retrieval uncertainty and bias at large
604 SZA can include atmospheric conditions, surface roughness and shadowing effects, surface structure,
605 detector response, and algorithmic assumptions. A better long-term solution might involve changes to
606 the MODIS retrieval algorithms that could be applied globally at large SZA, might require improved
607 characterization of atmospheric and surface conditions, or all of the above. The last decade of MODIS
608 snow-albedo retrievals constitutes an irreplaceable record of the status of and changes in surface snow
609 properties worldwide and it is hoped that these and future improvements to the accuracy of that record
610 will improve monitoring and evaluation of cryospheric change well into the second decade of MODIS.

611

612

613 **Acknowledgments.** We thank all researchers who installed and maintain the GC-Net AWS stations
614 that provide the calibrated *in-situ* radiative fluxes upon which this work is based. We also thank the
615 MODIS albedo science team and the Land Processes Distributed Active Archive Center (LP DAAC))
616 for providing the MCD43C albedo data. We thank C. Schaaf, A. Strahler, Z. Wang, two anonymous
617 reviewers and the editors for their helpful comments which greatly improved this manuscript. Funding
618 for this work is provided by NASA International Polar Year (IPY) Program, NASA NNX07AR23G
619 and NSF ARC-0714088.

620

621 **References:**

- 622
- 623 Augustine, J. A., J. DeLuise, and C. Long. 2000. SURFRAD: A national surface radiation budget
624 network for atmospheric research, *Bull. Am. Meteorol. Soc.*, 81, 2341–2357.
- 625 Box J. and K. Steffen. November 10, 2000. Online article: Greenland climate network (GC-NET) Data
626 Reference; retrieved on December 12, 2008 at:
627 <http://cires.colorado.edu/science/groups/steffen/gcnet/>.
- 628 Briegleb, B.P., P. Minnis, V. Ramanathan and E. Harrison. 1986. Comparison of regional clear sky
629 albedos inferred from satellite observations and model calculations. *J. Clim. Appl. Meteorol.*, 25,
630 214 – 226.
- 631 Carroll, J.J. And B.W. Fitch. 1981. Effects of solar elevation and cloudness on snow albedo at the
632 South Pole. *J. Geophys. Res.*, 86, 5271-5276.
- 633 Dickinson, R.E., 1983. Land surface processes and climate-surface albedos and energy balance.
634 *Advance in Geophysics*, 25, 305-353.
- 635 Flanner, M. G., and C. S. Zender. 2006. Linking Snowpack Microphysics and Albedo Evolution, *J.*
636 *Geophys. Res.*, 111(D12), D12208, doi:10.1029/2005JD006834.
- 637 Flanner, M.G., C.S. Zender, J.T. Randerson, P.J. Rasch. 2007. Present-day climate forcing and
638 response from black carbon in snow. *J. Geophys. Res.*, 112, D11202, doi:10.1029/2006JD008003.
- 639 Flanner, M.G., C.S. Zender, P.G. Hess, N.M. Mahowald, T.H. Painter, V. Ramanathan and P.J. Rasch.
640 2009. Springtime warming and reduced snow cover from carbonaceous particles. *Atmos. Chem.*
641 *Phys.*, 9, 2481–2497, 2009.
- 642 Greuell, W., and J. Oerlemans. 2005. Validation of AVHRR- and MODIS-derived albedos of snow and
643 ice surfaces by means of helicopter measurements. *Journal of Glaciology*, 51(172), 37–48.
- 644 Hou, Y.T., S. Moorthi and K. Campana. 2002. Parameterization of solar radiation transfer in the NCEP
645 models. NCEP Off. Note 441, 34 pp., National Center for Environmental Prediction, Camp springs,
646 Maryland.
- 647 Jin, Y., C. B. Schaaf, F. Gao, X. Li, A. H. Strahler, W. Lucht, and S. Liang. 2003a. Consistency of
648 MODIS surface bidirectional reflectance distribution function and albedo retrievals: 1. Algorithm
649 performance. *J. Geophys. Res.*, 108(D5), 4158, doi:10.1029/2002JD002803, 2003.
- 650 Jin, Y., C. B. Schaaf, C. E. Woodcock, F. Gao, X. Li, A. H. Strahler, W. Lucht, and S. Liang . 2003b.
651 Consistency of MODIS surface bidirectional reflectance distribution function and albedo retrievals:
652 2. Validation. *J. Geophys. Res.*, 108(D5), 4159, doi:10.1029/2002JD002804.
- 653 Jin, Z., T.P. Charlock, P. Yang, Y. Xie, and W. Miller. 2008. Snow optical properties for different
654 particle shapes with application to snow grain size retrieval and MODIS/CERES radiance
655 comparison over Antarctica. *Remote Sensing of Environment*, 112, 3563-3581.
- 656 Kiehl, J., J. Hack, G. B. Bonan, B. Bonville, D. L. Williamson, and P. J. Rasch. 1998. The national
657 center for atmospheric research community climate model: CCM3. *Journal of Climate*, 11, 1131 –
658 1149.
- 659 Knap, W. H. and J. Oerlemans. 1996. The surface albedo of the Greenland ice sheet: satellite-derived

660 and in situ measurements in the Søndre Strømfjord area during the 1991 melt season. *Journal of*
661 *Glaciology*, 42, 364–374.

662 Koch, D., and J. Hansen. 2005. Distant origins of Arctic black carbon: A Goddard Institute for Space
663 Studies ModelE experiment. *J. Geophys. Res.*, 110, D04204, doi:10.1029/2004JD005296.

664 Kuhn, M. and L. Siogas. 1978. Spectroscopic studies at McMurdo, South Pole and Siple Stations
665 during the austral summer 1977-78. *Antarctic J. U.S.*, 13, 178-179.

666 Lewis, P., and M. J. Barnsley (1994), Influence of the sky radiance distribution on various formulations
667 of the Earth surface albedo, paper presented at International Symposium on Physical Measurements
668 and Signatures in Remote Sensing, *Int. Soc. for Photogramm. and Remote Sens.*, Val d'Isere,
669 France.

670 Liu, J., C. Schaaf, A. Strahler, Z. Jiao, Y. Shuai, Q. Zhang, M. Roman, J. A. Augustine, and E. G.
671 Dutton. 2009. Validation of Moderate Resolution Imaging Spectroradiometer (MODIS) albedo
672 retrieval algorithm: Dependence of albedo on solar zenith angle. *J. Geophys. Res.*, 114, D01106,
673 doi:10.1029/2008JD009969.

674 Lucht, W. 1998. Expected retrieval accuracies of bidirectional reflectance and albedo from EOS-
675 MODIS and MISR angular sampling. *J. Geophys. Res.*, 103, 8763 – 8778.

676 Ming, J., C. Xiao, H. Cachier, D. Qin, X. Qin, Z. Li and J. Pu. 2009. Black Carbon (BC) in the snow of
677 glaciers in west China and its potential effects on albedos. *Atmospheric Research*, 92, 114–123.

678 Oleson, K. W., G. B. Bonan, C. B. Schaaf, F. Gao, Y. Jin, and A. Strahler, Assessment of global climate
679 model land surface albedo using MODIS data. *Geophys. Res. Lett.*, 30(8), 1443,
680 doi:10.1029/2002GL016749, 2003.

681 Painter, T. H., A.P. Barrett, C.C. Landry, J.C. Neff, M.P. Cassidy, C.R. Lawrence, K.E. McBride and
682 G.L. Farmer: Impact of disturbed desert soils on duration of mountain snow cover. *Geophys. Res.*
683 *Lett.*, 34, L12502, doi:10.1029/2007GL030284, 2007.

684 Petzold, D.E. 1977. An estimation technique for snow surface albedo. *Clim. Bull.*, 21, 1-11.

685 Pinker, R.T. and I. Laszlo. 1992. Modeling of surface solar irradiance for satellite applications on a
686 global scale. *J. Appl. Meteorol.*, 31, 194 – 211.

687 Roesch, A., C. B. Schaaf. and F. Gao. 2004. Use of Moderate-Resolution Imaging Spectroradiometer
688 bidirectional reflectance distribution function products to enhance simulated surface albedo. *J.*
689 *Geophys. Res.*, 109, D12105, doi:10.1029/2004JD004552.

690 Roesch, A. 2006. Evaluation of surface albedo and snow cover in AR4 coupled climate models. *J.*
691 *Geophys. Res.*, 111, D15111, doi:10.1029/2005JD006473.

692 Salomon, J.G., C.B. Schaaf, A.H. Strahler, F. Gao, Y. Jin. 2006. Validation of the MODIS
693 Bidirectional Reflectance Distribution Function and Albedo Retrievals Using Combined
694 Observations From the Aqua and Terra Platforms. *IEEE TRANSACTIONS ON GEOSCIENCE AND*
695 *REMOTE SENSING*, 44, 1555-1565, DOI:10.1109/TGRS.2006.871564.

696 Schaaf, C.B., F. Gao, A. Strahler, W. Lucht, X. Li, T. Tsang, N.C. Strugnell, X. Zhang, Y. Jin, J.-P.
697 Muller, P. Lewis, M. Barnsley, P. Hobson, M. Disney, G. Roberts, M. Underdale, C. Doll, R.P.,
698 d'Entremont, B. Hu, S. Liang, J.L. Privette, D. Roy. 2002. First operational BRDF, albedo nadir

699 reflectance products from MODIS. *Remote Sensing of Environment*, 83, 135-148.

700 Steffen, K. and J. Box. 2001. Surface climatology of the Greenland Ice Sheet: Greenland climate net-
701 work 1995-1999. *J. Geophys. Res.*, 106, No. D24, Pages 33,951-33,964, December 2001.

702 Stroeve, J.C., A. Nolin and K. Steffen. 1997. Comparison of AVHRR-derived and in situ surface
703 albedo over the Greenland Ice Sheet. *Remote Sensing of Environment*, 62, 262-276.

704 Stroeve, J.C., J.E. Box, C. Fowler, T. Haran and J. Key. 2001. Intercomparison between in situ and
705 AVHRR polar pathfinder-derived surface Albedo over Greenland. *Remote Sensing of Environment*,
706 75, 360-374

707 Stroeve, J., J.E. Box, F. Gao, S. Liang, A. Nolin, C. Schaaf. 2005. Accuracy assessment of the MODIS
708 16-day albedo product for snow: comparisons with Greenland in situ measurements. *Remote*
709 *Sensing of Environment*, 94, 46-60, doi:10.1016/j.rse.2004.09.001.

710 Stroeve, J.C., J.E. Box and T Haran. 2006. Evaluation of the MODIS(MOD10A1) daily snow albedo
711 product over the Greenland ice sheet. *Remote Sensing of Environment*, 105, 155-171.

712 Sturm, M., J. Holmgren and G. E. Liston. 1995. A seasonal snow cover classification system for local
713 to global applications. *Journal of Climate*, 8(5):1261-1283.

714 Tedesco, M. 2007. Snowmelt detection over the Greenland ice sheet from SSM/I brightness
715 temperature daily variations. *Geophysical Research Letters*, 34, L02504,
716 doi:10.1029/2006GL028466, 2007.

717 Wang, K., J. Liu, X. Zhou, M. Sparrow, M. Ma, Z. Sun and W. Jiang. 2004. Validation of the MODIS
718 global land surface albedo product using ground measurements in a semidesert region on the Tibetan
719 Plateau, *J. Geophys. Res.*, 109, D05107, doi:10.1029/2003JD004229.

720 Wang, Z., M. Barlage, X. Zeng, R.E. Dickinson and C.R. Schaaf. 2005. The solar zenith angle
721 dependence of desert albedo. *Geophysical Research Letter*, 32, L0543,
722 doi:10.1029/2004GL021835.

723 Wang, X. and C. Zender. 2010. MODIS albedo bias at high zenith angle relative to theory and to in situ
724 observations in Greenland. *Remote Sensing of Environment*, 114, 563-575.

725 Wang X, H. Xie and T. Liang. 2008. Evaluation of MODIS snow cover and cloud mask and its
726 application in Northern Xinjiang, China. *Remote Sensing of Environment*, 112, 1497-1513.

727 Warren, S.G. 1982. Optical properties of snow. *Review of Geophysics and space Physics*, 20, 67-89.

728 Warren, S.G. and W.J. Wiscombe. 1980. A model for the spectral albedo of snow. II: snow containing
729 atmospheric aerosols. *Journal of the Atmospheric Sciences*, 37, 2734-2745.

730 Wielicki, B. A., B. R. Barkstrom, E. F. Harrison, R. B. Lee, G. L. Smith and J. E. Copper. 1985.
731 Clouds and the Earth's Radiant Energy System (CERES): An Earth Observing System Experiment.
732 *Bull. Amer. Meteo. Soc.*, 77.

733 Wiscombe, W.J. and S.G. Warren. 1980. A model for the spectral albedo of snow. I: pure snow.
734 *Journal of the Atmospheric Sciences*, 37, 2712-2733.

735 Zhou, L. R.E. Dickinson, Y. Tian, X. Zeng, Y. Dai, Z.-L. Yang, C.B. Schaaf, F. Gao, Y. Jin, A.
736 Strahler, R.B. Myneni, H. Yu, W. Wu and M. Shaikh. 2003. Comparison of seasonal and spatial

737 variations of albedos from Moderate-Resolution Imaging Spectroradiometer (MODIS) and Common
738 Land Model. *J. Geophys. Res.*, 108(D15), 4488, doi:10.1029/2002JD003326.

739 Figure Captions

740

741 Figure 1. Location and elevation of the Greenland Climate Network (GC-Net) Automatic Weather
742 Stations (AWS) (plus symbols). The five red-shaded stations are selected in this study. These stations
743 are located along the crest of the ice sheet facies and transect Greenland from south to north at
744 elevations close to and above 2000 m, where snow cover is perennial and dry.

745

746 Figure 2. Cosine(SZA) and MODIS black sky shortwave albedo (all retrievals) in spring (left panel)
747 and in fall (right panel) at the Summit station from 2003-2007.

748

749 Figure 3. Correlation coefficient R (blue columns) between $\cos(\text{SZA})$ and the zonal mean MODIS
750 black-sky snow albedo (all retrievals) in Greenland from 50°W-40°W averaged into 1° latitude bands
751 from 65°N to 80°N. Filled blue columns represent significant correlation at 0.95 confidence level. Red
752 columns are the albedo difference ($\text{alb}_{65\text{N}}$ minus $\text{alb}_{80\text{N}}$) between zonal mean albedo at latitude
753 65°N and at 80°N. The two green curves show the noontime SZA (using the right hand vertical axis) at
754 latitudes 65°N and 80°N.

755

756 Figure 4. Monthly CERES (a) and MODIS (b) black-sky snow albedo and their difference (c) and the
757 corresponding difference implied in surface absorbed solar radiation (d) in Greenland in March, 2005.
758 The CERES and MODIS mean albedos are conditional flux and area-weighted means for gridpoints
759 with MODIS albedo >0.5 to focus on snow-covered areas only. CERES data were simply resampled
760 from the 1° CERES grid onto 0.05° MODIS grid. The monthly area-weighted CERES-estimated
761 surface insolation over Greenland is 89W/m² in March, 2005.

762

763 Figure 5. Reference albedo ($\bar{A} \equiv \text{Ref_albd_Q0}$), number of $Q=0$ gridpoints (right hand-side axis)
764 used to calculate the reference albedo (Ref_cells), and mean albedo at 63°N ($\bar{A}(63\text{N}) \equiv$
765 Ref_albd_63N) for white-sky (A. WSA) and black-sky albedo (B. BSA) in 2005.

766

767 Figure 6. Comparison of MODIS raw (WSA/BSA_raw) and two adjusted albedos based on the final
768 reference albedos (WSA/BSA_new) and the uncorrected reference albedos at 63°N
769 (WSA/BSA_new_63N), and the AWS measured albedo at Summit in 2005. The right hand-side
770 vertical axis shows the SZA in degrees.

771

772 Figure 7. Comparison of MODIS raw (shortwave WSA/BSA) and four corrected albedos based on
773 different C values in Equation (2) along a south-to-north (62-80°N) transect in central Greenland
774 (45°W) on day 73, 2005, when the SZA approximately equals to the latitude in degrees. The red
775 dotted line shows the raw MODIS albedo. The four solid lines show adjusted albedos using C values
776 of 0.1, 0.15, 0.2 and 0.3, respectively from bottom to top. The solid green line ($C = 0.15$) is our best-
777 estimate adjusted snow albedo along the transect.

778

779 Figure 8. Comparison of GC-Net measured albedo and MCD43C3 raw and adjusted (new) albedo at the
780 Saddle (SDL, A) and Summit stations (SMM, B) for all available GC-Net data in the five years from
781 2003 to 2007 on days when the SZA is less than 75°. The right hand-side vertical axis shows the solar

782 zenith angle (SZA) in degrees. The albedo adjustments are applied before day 97 and after day 249 at
783 Saddle, and before day 129 and after day 217 at Summit. The GC-Net measured snow albedos shown
784 have a mean positive bias of ~ 0.03 compared to more accurate Kipp and Zonen CM 21 pyranometer
785 measurements (not shown).

786 Figure 9. Raw (a, b, raw) and adjusted (c, d, new) MCD43C3 shortwave black-sky albedo in
787 Greenland on days 73 (March) and 105 (April), 2005. The SZAs at latitude 65° and 75° on day 73 are
788 65° and 75° , respectively, and on day 105 are 55° and 65° , respectively.

789

790 Figure 10. Monthly mean CERES (a) and adjusted MODIS (b) black-sky snow albedo, their difference
791 (c), and the corresponding difference implied in surface absorbed solar radiation (d) in Greenland in
792 March 2005. The area-weighted surface insolation over Greenland is 89 W/m^2 in March, 2005.
793 Differences were constructed from gridpoints with both MODIS and CERES albedo > 0.5 to exclude
794 non-snow covered areas.

795

796 Figure 11. Seasonal cycle of the potential maximum snow melt and sublimation in snow water
797 equivalent (SWE, cm) that would be produced by converting the MODIS absorbed solar radiation bias
798 (raw-new) in Greenland to melt or sublimation, respectively. The vertical whiskers on the SWE_melt
799 curve show the range of \pm one standard deviation (δ) uncertainty for each month computed from the
800 three years (2003-2005). Surface solar insolation is obtained from CERES estimates. The right hand-
801 side vertical axis is for albedo.

802

803 Figure 12. The potential maximum snow sublimation in March (a), April (b) and September (d) and
804 snow melt in August (c) in snow water equivalent (SWE, cm) due to converting the MODIS absorbed
805 solar radiation bias in 2005 (determined from black-sky albedo) entirely to snow melt or to
806 sublimation. Surface solar insolation is obtained from CERES estimates.

807

808

809

810 Table 1. Greenland Climate Network (GC-Net) Automatic Weather Stations (AWS) used in this study
811 (Steffen and Box, 2001).

Station ID	Name	Latitude (N)	Longitude (W)	Elevation (m)	Start Date
05 (HMG)	Humboldt Gl.	78.5266	56.8305	1995	1995.47
14 (NGR)	NGRIP	75.0998	42.3326	2950	1997.52
06 (SMM)	Summit	72.5794	38.5042	3208	1996.37
10 (SDL)	Saddle	66.0006	44.5014	2559	1997.3
11 (SDM)	South Dome	63.1489	44.8167	2922	1997.31

813

814

815 Table 2. Mean monthly area-weighted land surface insolation flux (W/m^2), area and flux-weighted raw
 816 MODIS black-sky albedo, adjusted MODIS black-sky albedo, snow surface absorbed solar radiation
 817 (ASR) and ASR difference between adjusted (new) and original (raw) MODIS albedo, and percent
 818 differences relative to the insolation and the original MODIS snow albedo ASR on Greenland from
 819 2003 to 2005. Standard deviations of ASR differences are based on the three-year comparison.

820

Mean from 2003 to 2005	Downwelling solar radiation (W/m^2)	Raw MODIS albedo	Corrected MODIS albedo	ASR using raw MODIS albedo (W/m^2)	Mean ASR difference (New-Raw) (W/m^2)	Standard deviation of ASR difference	Relative ARS difference vs downwelling radiation (%)	Relative ASR difference vs raw ASR (%)
January	10	0.66	0.81	3.3	-1.4	0.3	-14.7%	-43.5%
February	29	0.7	0.8	8.8	-3.1	0.2	-10.7%	-35.3%
March	89	0.75	0.79	22.4	-4.1	0.5	-4.6%	-18.4%
April	214	0.78	0.8	46.2	-2.6	0.1	-1.2%	-5.6%
May	337	0.77	0.78	77.4	-3.3	0.8	-1.0%	-4.3%
June	400	0.75	0.75	99.4	-0.7	0.1	-0.2%	-0.7%
July	365	0.75	0.75	91.9	-2.5	0.5	-0.7%	-2.7%
August	253	0.77	0.79	59.0	-5.4	1.6	-2.1%	-9.1%
Septembe	131	0.76	0.81	31.1	-6.2	0.9	-4.7%	-19.8%
October	40	0.7	0.8	11.8	-4.0	0.5	-10.0%	-33.8%
November	14	0.65	0.81	4.9	-2.3	0.3	-16.5%	-47.0%
December	9	0.63	0.83	3.2	-1.2	0.2	-13.9%	-37.3%
Annual	158	0.76	0.78	38.3	-3.1	0.2	-1.9%	-8.0%

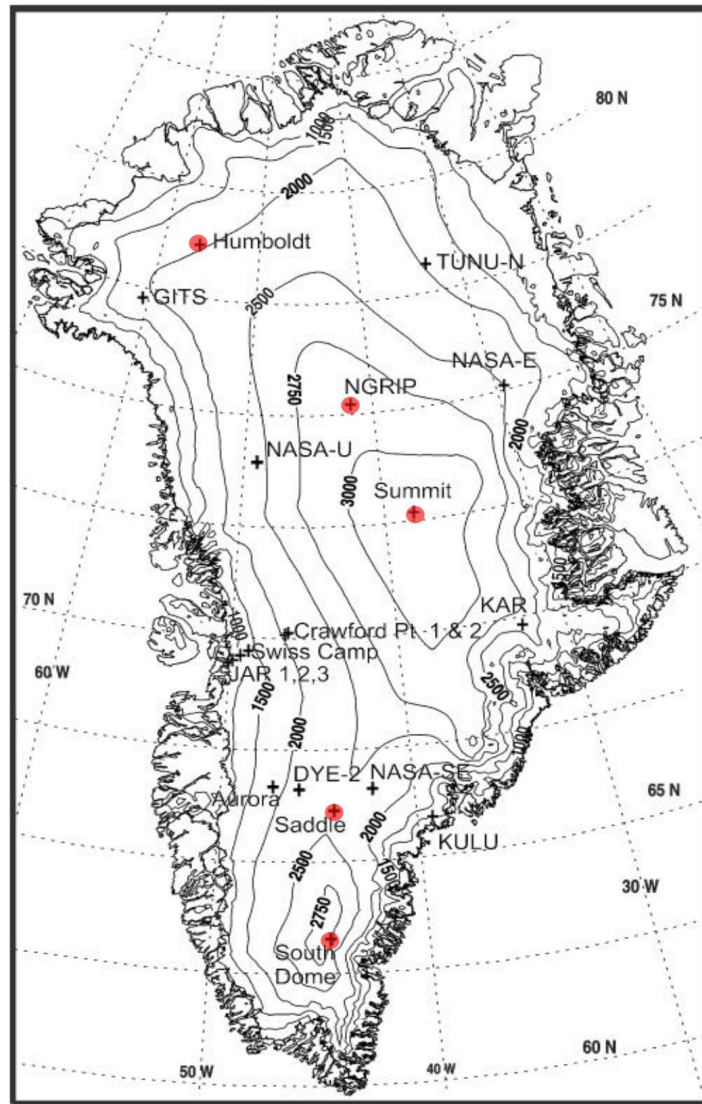


Figure 1. Location and elevation of the Greenland Climate Network (GC-Net) Automatic Weather Stations (AWS) (plus symbols). The five red-shaded stations are selected in this study. These stations are located along the crest of the ice sheet facies and transect Greenland from south to north at elevations close to and above 2000 m, where snow cover is perennial and dry.

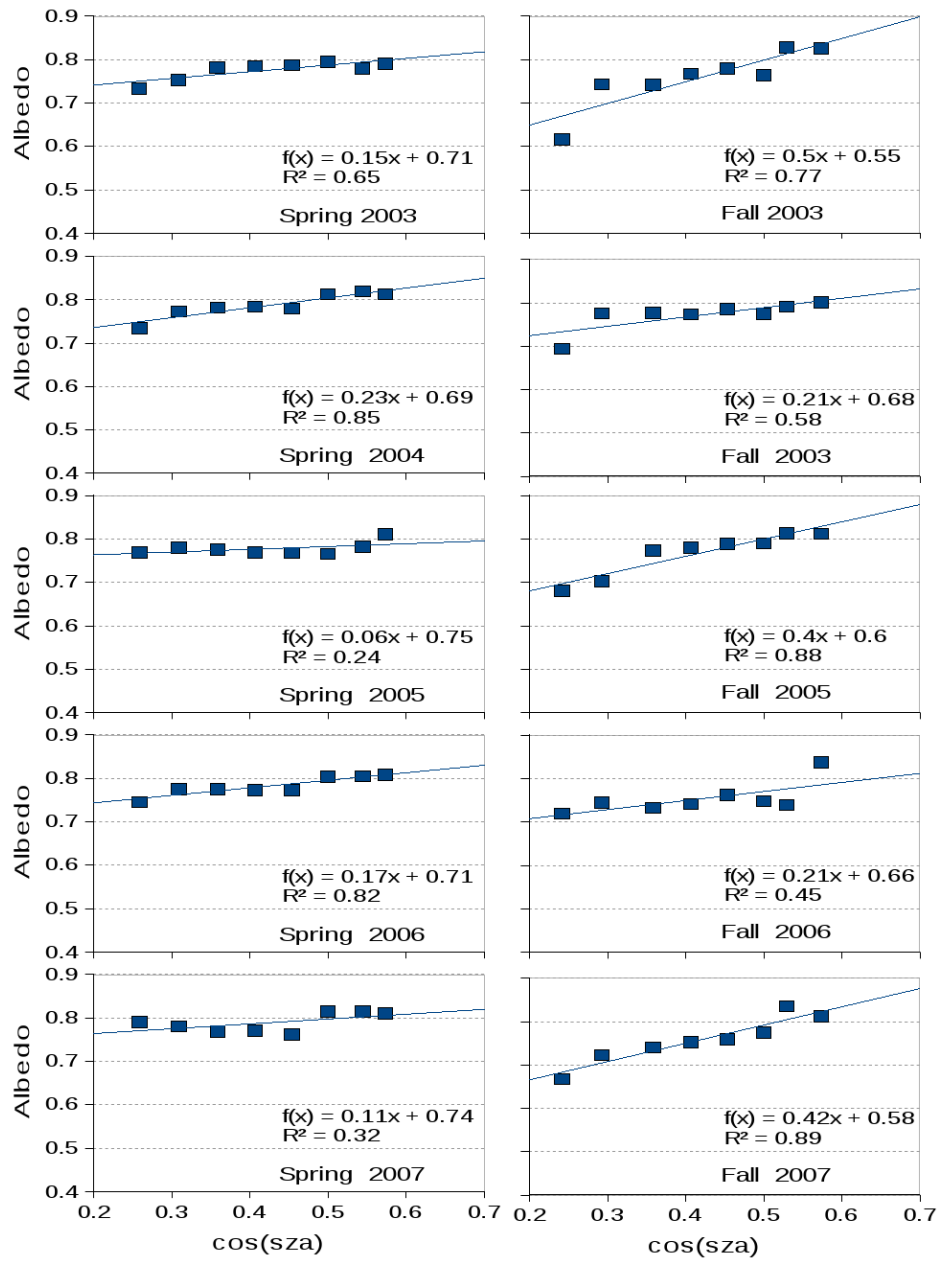
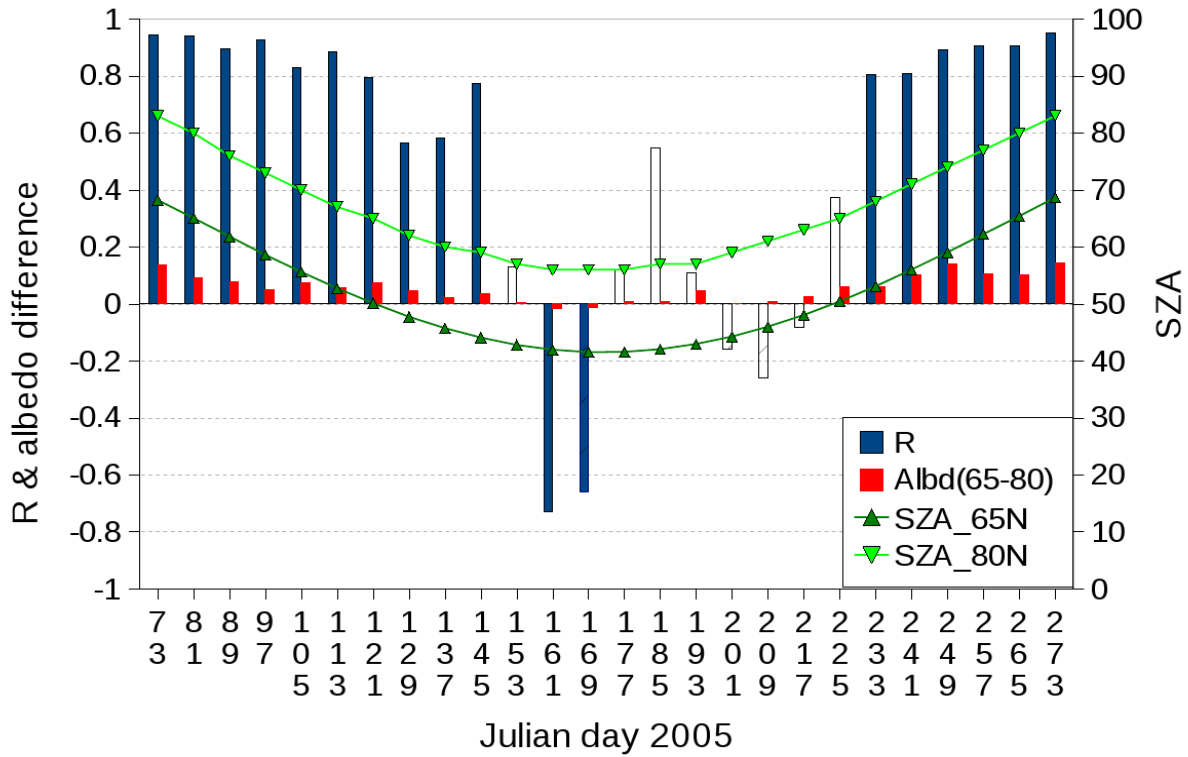
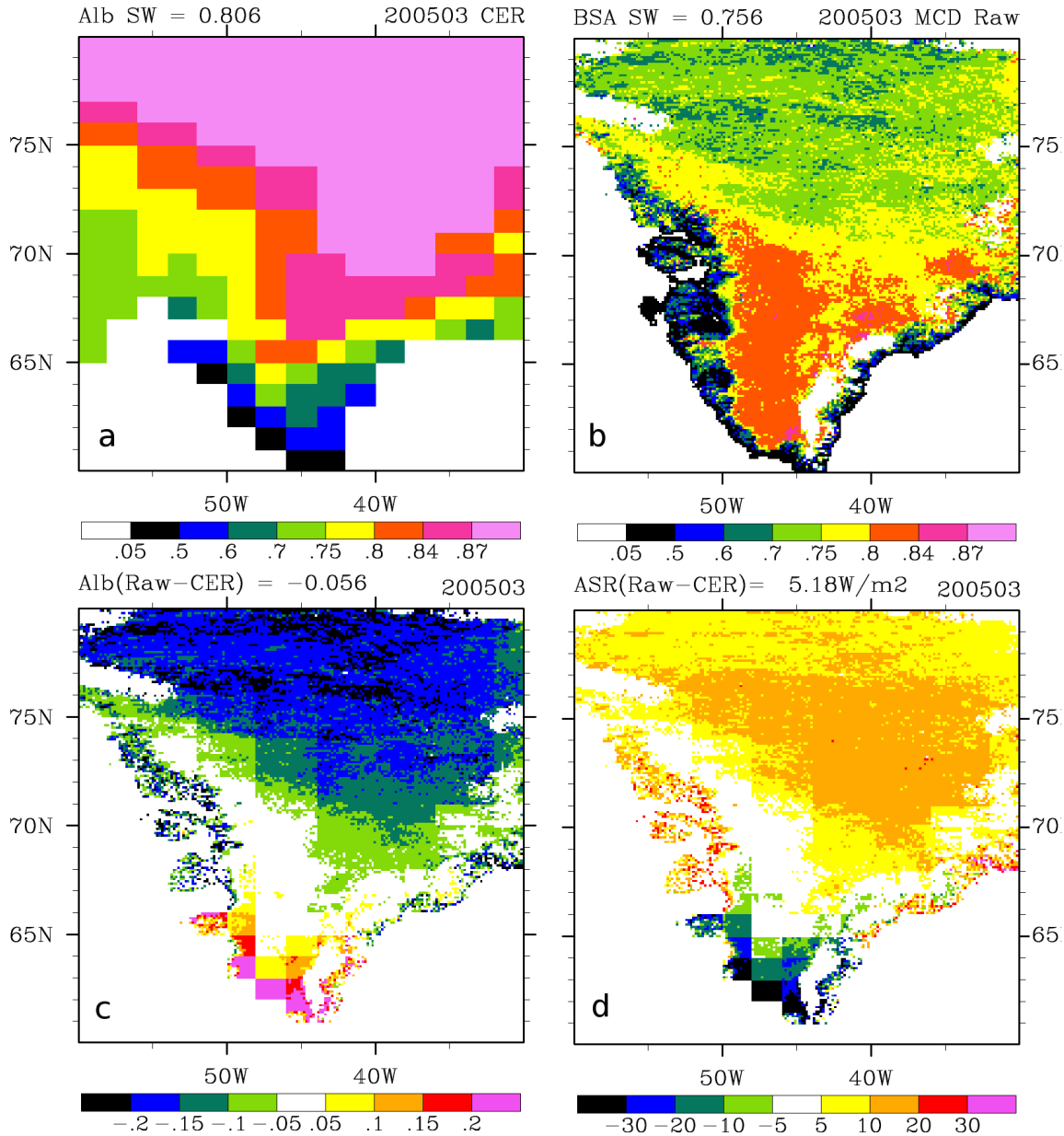


Figure 2. Cosine(SZA) and MODIS black sky shortwave albedo (all retrievals) in spring (left panel) and in fall (right panel) at the Summit station from 2003-2007.

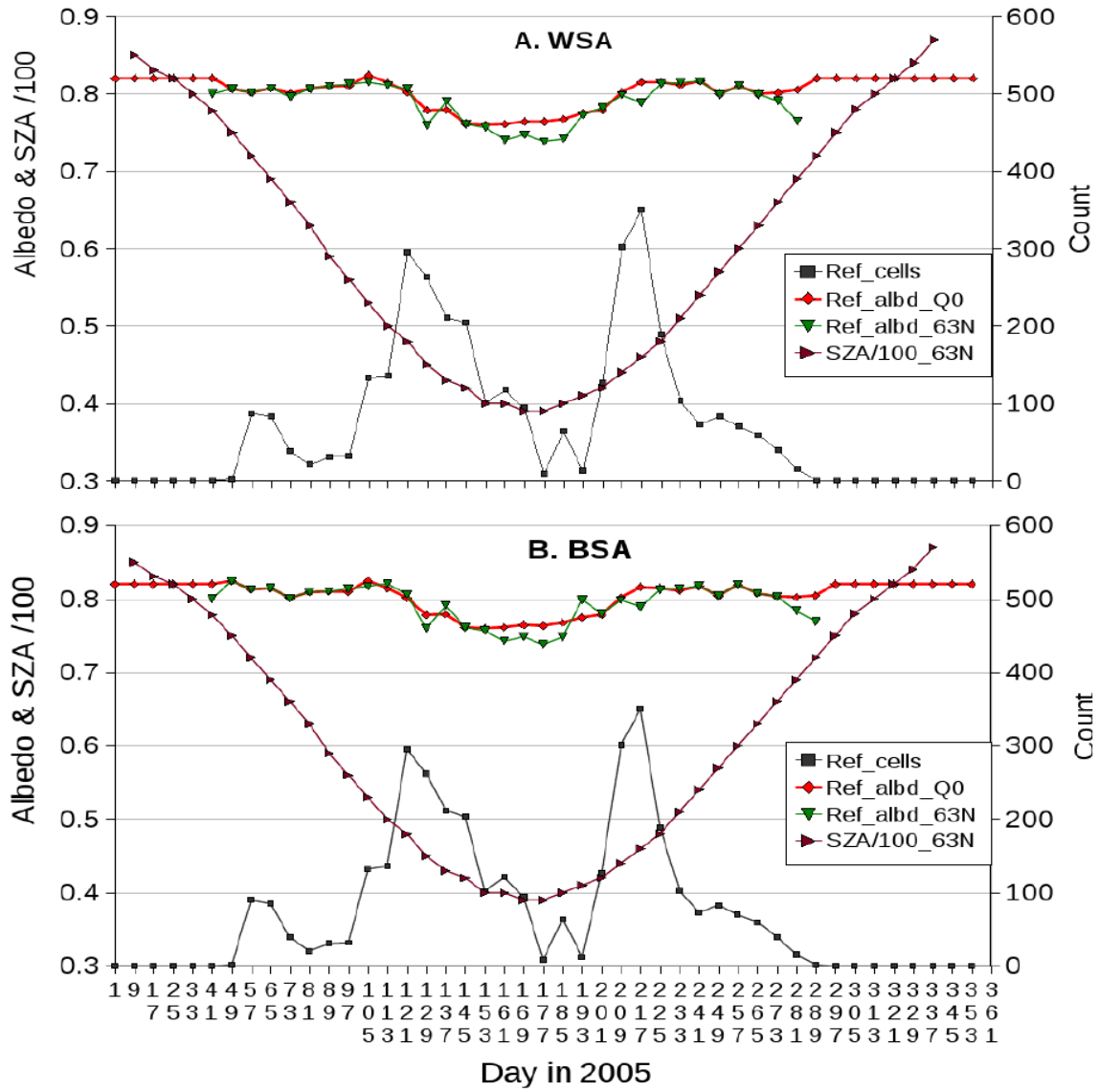


888 Figure 3. Correlation coefficient R (blue columns) between $\cos(\text{SZA})$ and the zonal mean MODIS
889 black-sky snow albedo (all retrievals) in Greenland from 50°W-40°W averaged into 1° latitude bands
890 from 65°N to 80°N. Filled blue columns represent significant correlation at 0.95 confidence level. Red
891 columns are the albedo difference (alb_65N minus alb_80N) between zonal mean albedo at latitude
892 65°N and at 80°N. The two green curves show the noontime SZA (using the right hand vertical axis) at
893 latitudes 65°N and 80°N.

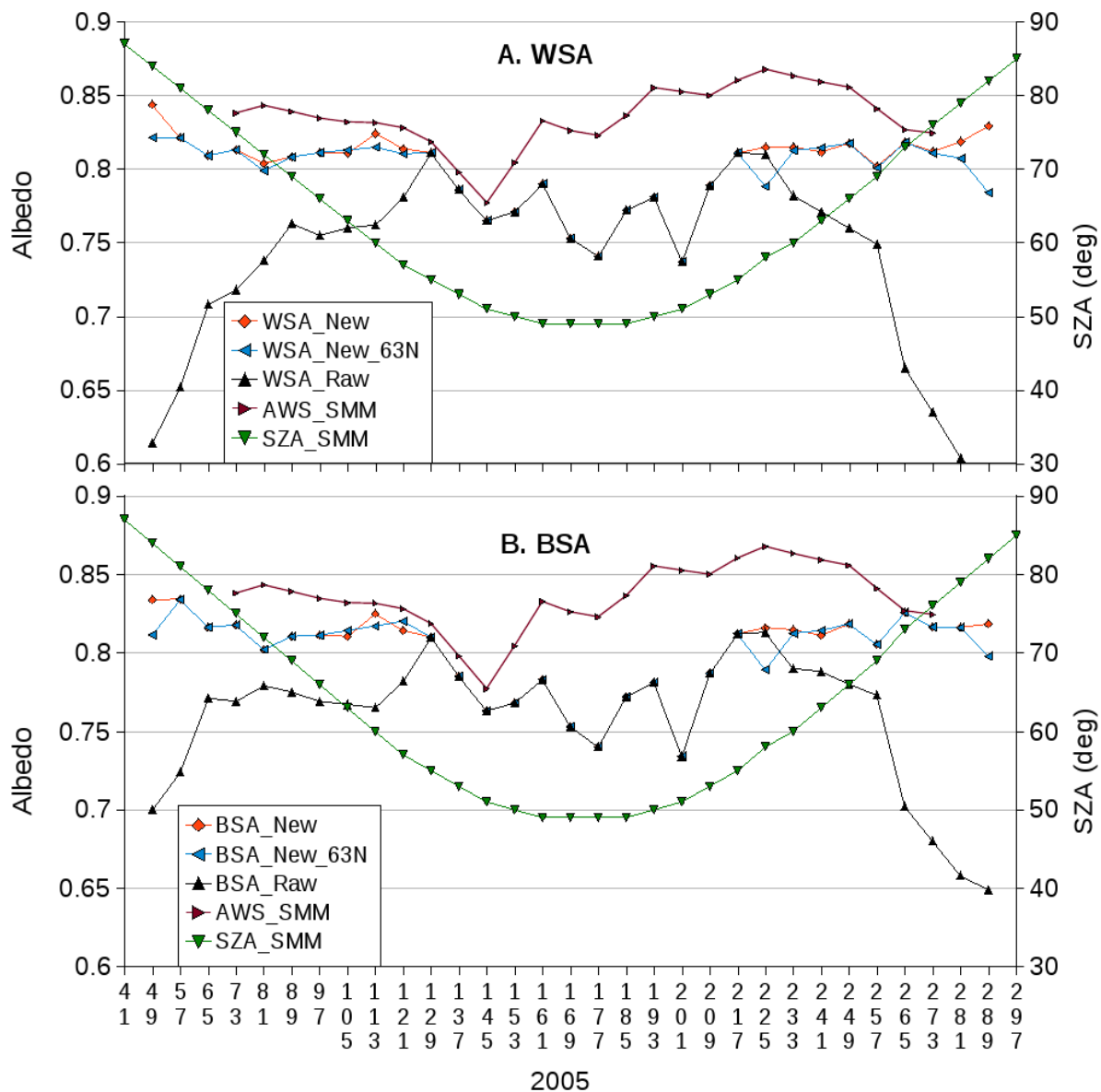
894



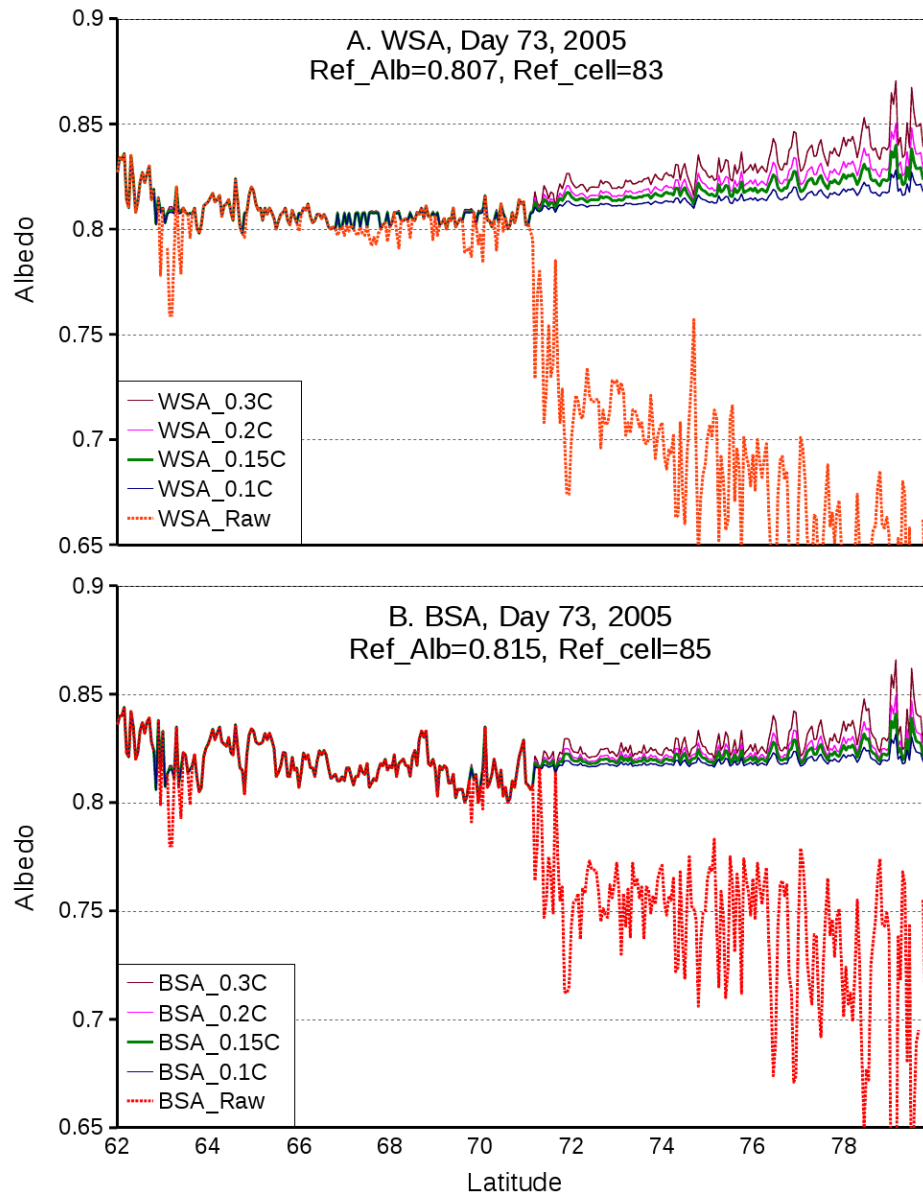
896 Figure 4. Monthly CERES (a) and MODIS (b) black-sky snow albedo and their difference (c) and the
 897 corresponding difference implied in surface absorbed solar radiation (d) in Greenland in March, 2005.
 898 The CERES and MODIS mean albedos are conditional flux and area-weighted means for gridpoints
 899 with MODIS albedo >0.5 to focus on snow-covered areas only. CERES data were simply resampled
 900 from the 1° CERES grid onto 0.05° MODIS grid. The monthly area-weighted CERES-estimated
 901 surface insolation over Greenland is 89W/m² in March, 2005.
 902



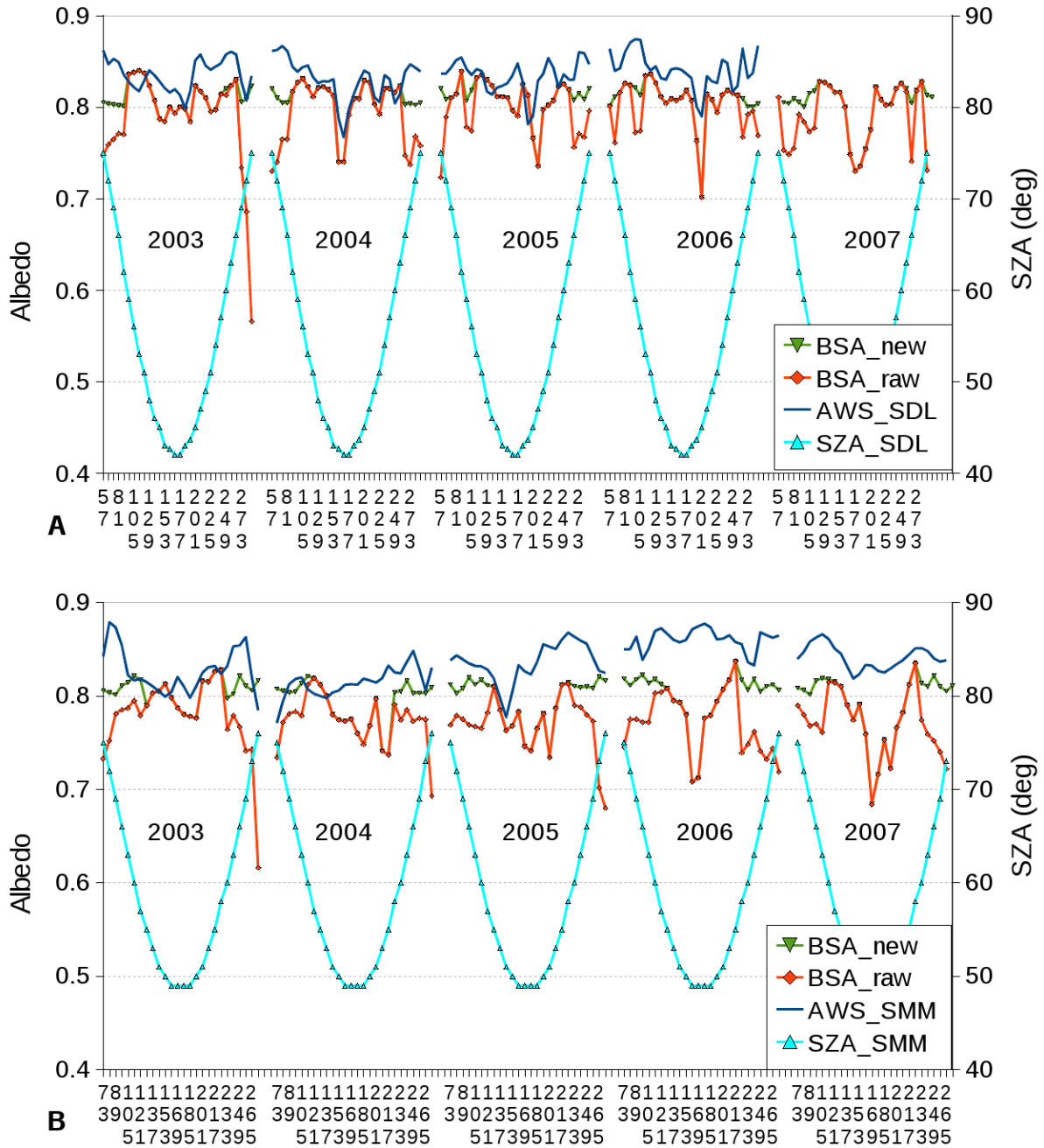
903 Figure 5. Reference albedo ($\bar{A}_0 \equiv \text{Ref_albd_Q0}$), number of Q=0 gridpoints (right hand-side axis)
 904 used to calculate the reference albedo (Ref_cells), and mean albedo at 63°N ($\bar{A}(63\text{N}) \equiv$
 905 Ref_albd_63N) for white-sky (A. WSA) and black-sky albedo (B. BSA) in 2005.



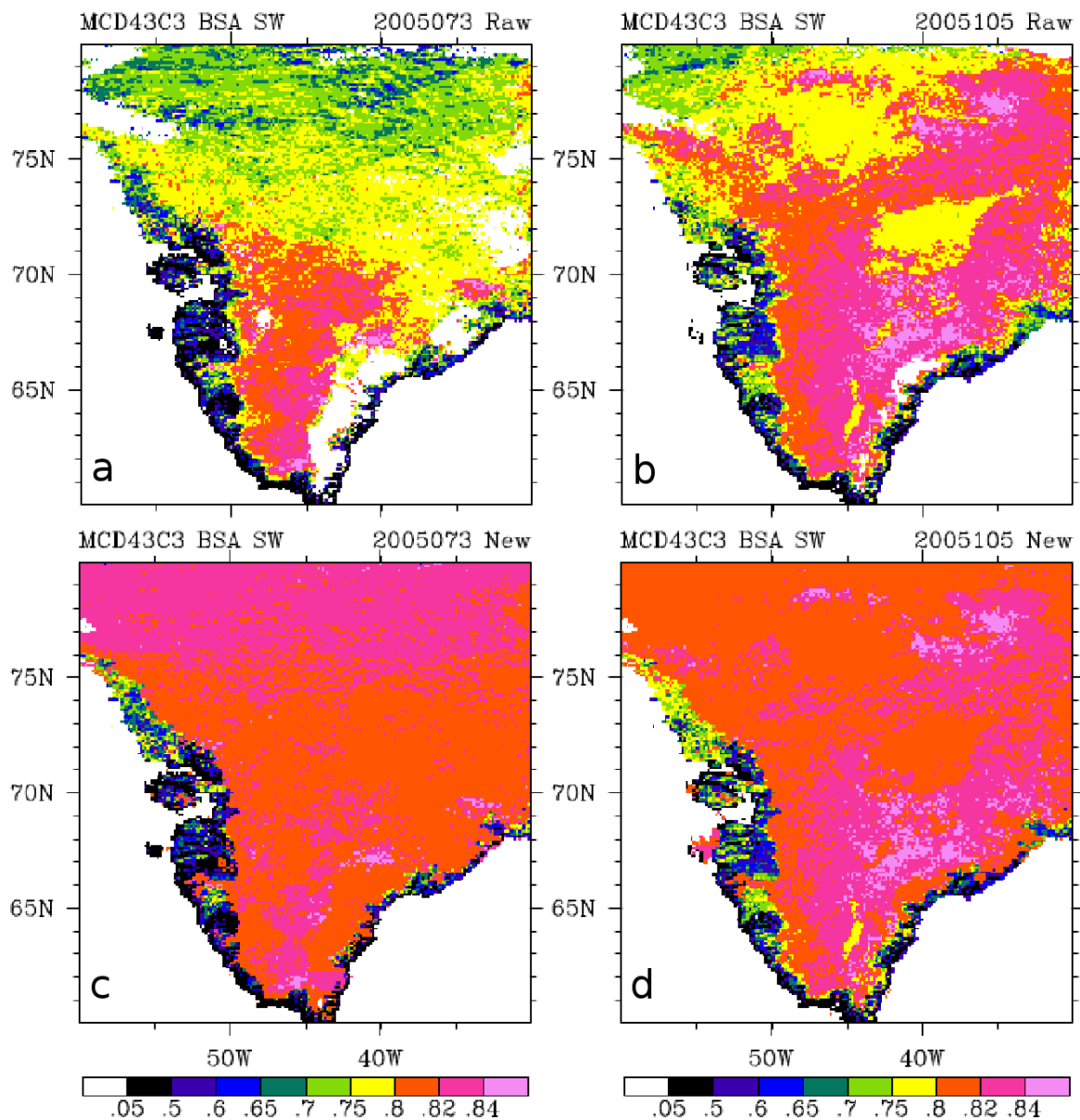
906 Figure 6. Comparison of MODIS raw (WSA/BSA_raw) and two adjusted albedos based on the final
 907 reference albedos (WSA/BSA_new) and the uncorrected reference albedos at 63°N
 908 (WSA/BSA_new_63N), and the AWS measured albedo at Summit in 2005. The right hand-side
 909 vertical axis shows the SZA in degrees.
 910



912 Figure 7. Comparison of MODIS raw (shortwave WSA/BSA) and four corrected albedos based on
 913 different C values in Equation (2) along a south-to-north (62-80°N) transect in central Greenland
 914 (45°W) on day 73, 2005, when the SZA approximately equals to the latitude in degrees. The red
 915 dotted line shows the raw MODIS albedo. The four solid lines show adjusted albedos using C values of
 916 0.1, 0.15, 0.2 and 0.3, respectively from bottom to top. The solid green line (C = 0.15) is our best-
 917 estimate adjusted snow albedo along the transect.

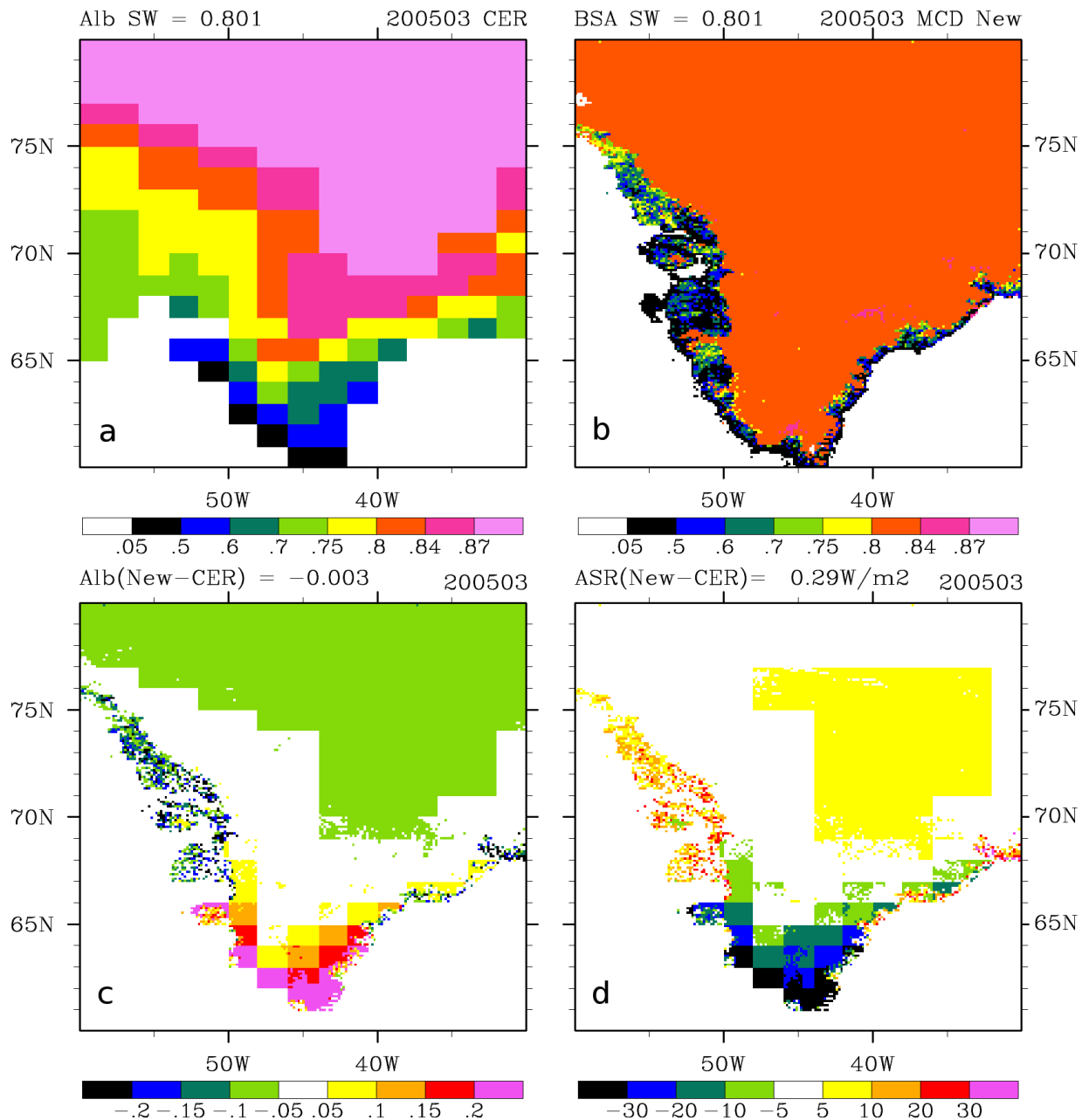


918 Figure 8. Comparison of GC-Net measured albedo and MCD43C3 raw and adjusted (new) albedo at the
919 Saddle (SDL, A) and Summit stations (SMM, B) for all available GC-Net data in the five years from
920 2003 to 2007 on days when the SZA is less than 75°. The right hand-side vertical axis shows the solar
921 zenith angle (SZA) in degrees. The albedo adjustments are applied before day 97 and after day 249 at
922 Saddle, and before day 129 and after day 217 at Summit. The GC-Net measured snow albedos shown
923 have a mean positive bias of ~0.03 compared to more accurate Kipp and Zonen CM 21 pyranometer
924 measurements (not shown).

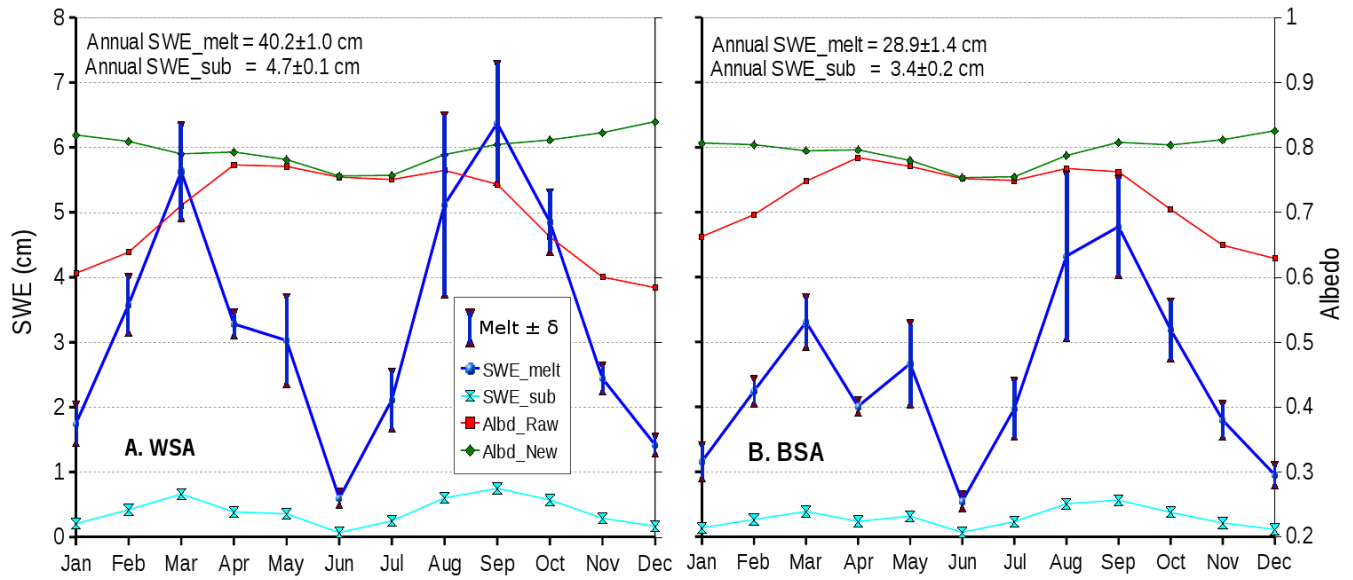


926 Figure 9. Raw (a, b, raw) and adjusted (c, d, new) MCD43C3 shortwave black-sky albedo in
 927 Greenland on days 73 (March) and 105 (April), 2005. The SZAs at latitude 65° and 75° on day 73 are
 928 65° and 75°, respectively, and on day 105 are 55° and 65°, respectively.

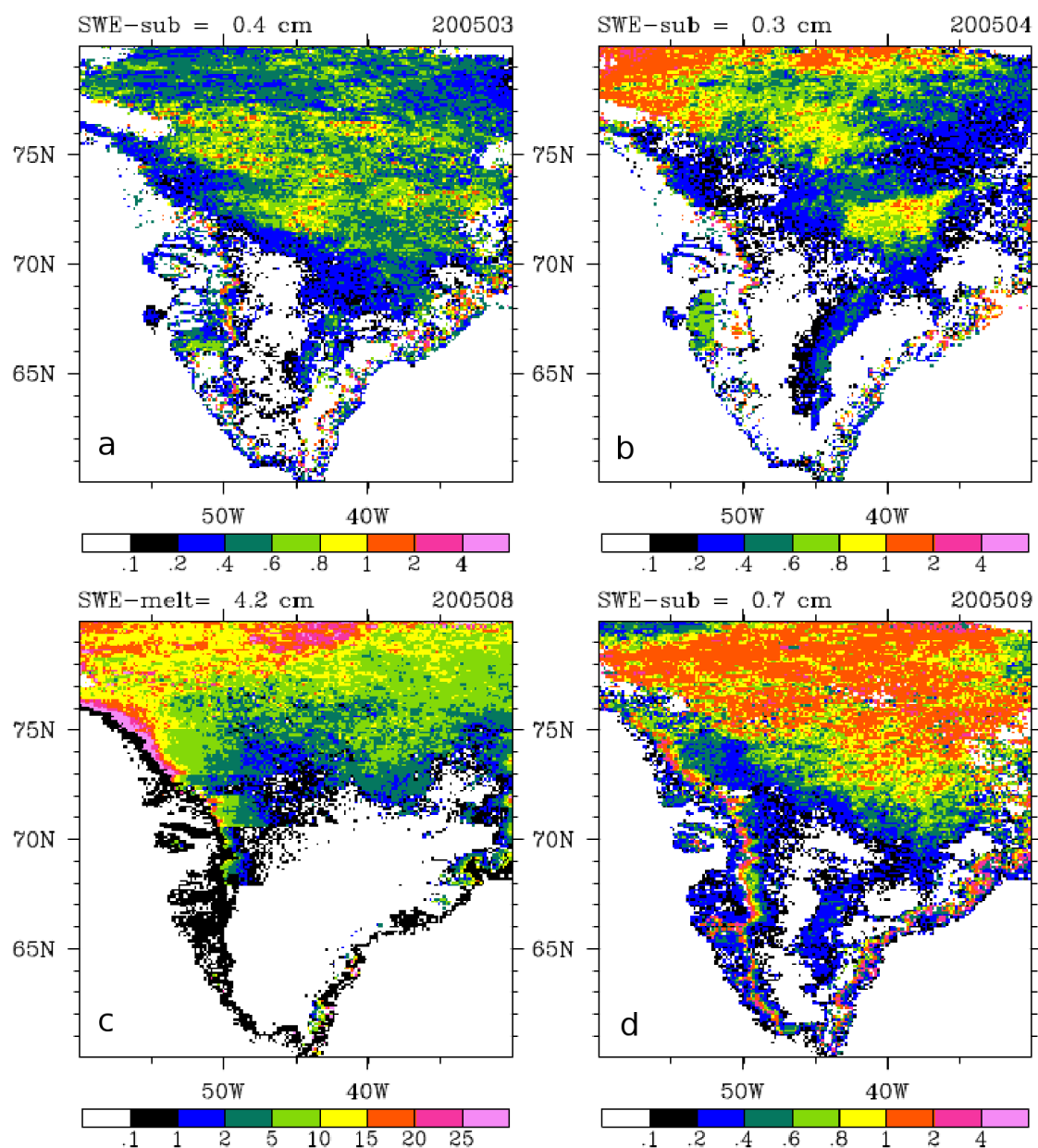
929
 930
 931
 932
 933
 934
 935
 936



938 Figure 10. Monthly mean CERES (a) and adjusted MODIS (b) black-sky snow albedo, their difference
 939 (c), and the corresponding difference implied in surface absorbed solar radiation (d) in Greenland in
 940 March, 2005. The area-weighted surface insolation over Greenland is 89 W/m² in March, 2005.
 941 Differences were constructed from gridpoints with both MODIS and CERES albedo > 0.5 to exclude
 942 non-snow covered areas.



943 Figure 11. Seasonal cycle of the potential maximum snow melt and sublimation in snow water
 944 equivalent (SWE, cm) that would be produced by converting the MODIS absorbed solar radiation bias
 945 (raw-new) in Greenland to melt or sublimation, respectively. The vertical whiskers on the SWE_melt
 946 curve show the range of \pm one standard deviation (δ) uncertainty for each month computed from the
 947 three years (2003-2005). Surface solar insolation is obtained from CERES estimates. The right hand-
 948 side vertical axis is for albedo.
 949



951 Figure 12. The potential maximum snow sublimation in March (a), April (b) and September (d) and
 952 snow melt in August (c) in snow water equivalent (SWE, cm) due to converting the MODIS absorbed
 953 solar radiation bias in 2005 (determined from black-sky albedo) entirely to snow melt or to
 954 sublimation. Surface solar insolation is obtained from CERES estimates.
 955